Chapter 7
Performance-Based Seismic Design and Assessment of Bridges

Andreas J. Kappos

Abstract Current trends in the seismic design and assessment of bridges are discussed, with emphasis on two procedures that merit some particular attention, displacement-based procedures and deformation-based procedures. The available performance-based methods for bridges are critically reviewed and a number of critical issues are identified, which arise in all procedures. Then two recently proposed methods are presented in some detail, one based on the direct displacement-based design approach, using equivalent elastic analysis and properly reduced displacement spectra, and one based on the deformation-based approach, which involves a type of partially inelastic response-history analysis for a set of ground motions and wherein pier ductility is included as a design parameter, along with displacement criteria. The current trends in seismic assessment of bridges are then summarised and the more rigorous assessment procedure, i.e. nonlinear dynamic response-history analysis, is used to assess the performance of bridges designed to the previously described procedures. Finally some comments are offered on the feasibility of including such methods in the new generation of bridge codes.

7.1 Introduction

Performance-based seismic design (PBD) procedures, in particular displacement-based ones (DBD), are now well-established for buildings (Kappos 2010); however application of these concepts to bridges has been more limited, despite the fact that studies on the so-called 'direct' displacement-based design (DDBD) of bridge piers (Kowalsky et al. 1995) or even entire bridges (Calvi and Kingsley 1995) appeared in the mid-1990s. Notwithstanding the now recognised advantages of the DDBD procedure (Priestley et al. 2007), the fact remains that, in its current form, the procedure suffers from two significant disadvantages:

A.J. Kappos (✉)
Civil Engineering Department, City University London, London EC1V 0HB, UK
e-mail: Andreas.Kappos.1@city.ac.uk

A. Ansal (ed.), *Perspectives on European Earthquake Engineering and Seismology*,
Geotechnical, Geological and Earthquake Engineering 39,
DOI 10.1007/978-3-319-16964-4_7

- it is applicable to a class of bridges only, i.e. those that can be reasonably approximated by an equivalent single-degree-of-freedom (SDOF) system for calculating seismic demand
- even for this class the procedure is not deemed appropriate for the *final* design of the bridge (whereas it is a powerful tool for its *preliminary* design)

A key source of these disadvantages is the important role that higher modes play in the transverse response of bridges, even of some relatively short ones (Paraskeva and Kappos 2010), which complicates the proper assessment of the displaced shape of the bridge and the target displacement. It is noted that for systems such as multi-span bridges, the DDBD approach requires that the engineer properly define a target displacement profile (duly accounting for inelastic response), rather than just a single target displacement (as in the case of single-column bridges); this usually requires a number of iterations, which inevitably increases the complexity of the procedure.

There is little doubt that the aforementioned disadvantages are the key reason why, even today (about 20 years after they first appeared) DBD/DDBD procedures are not formally adopted by current codes; interestingly, in Appendix I of the SEAOC 1999 Blue Book (Ad Hoc Committee 1999), the first one to provide guidance for DBD of buildings (there are still no guidelines for DBD of bridges), it is explicitly required to carry out a verification of the initial displacement-based design through nonlinear static (pushover) analysis.

In the light of the above, it can be claimed that the current trend in performance-based seismic design of bridges is to make the attractive concept of DBD more suitable for the final design of a sufficiently broad class of bridges, so that it can be deemed suitable for practical application. It is worth recalling here that, as correctly pointed out in one of the first papers on DDBD (Calvi and Kingsley 1995), the concept of the equivalent elastic structure (based on member secant stiffness at target displacement) is feasible and preferable in the preliminary design of the bridge, whereas more sophisticated tools (like nonlinear analysis) are recommended at the final design stage. As will be discussed in more detail in Sect. 7.3, the currently available DDBD procedures work well for the preliminary design of first-mode-dominated bridges in high seismic hazard areas, but present problems in several cases that are common in practice, like bridges with some degree of irregularity, while they are simply not applicable in low and moderate seismic hazard regions.

In Sect. 7.2 a brief overview of available PBD/DBD methods for bridges is critically presented, focussing on the new contributions made by each study, rather than summarising the entire procedures (which are similar in many methods). The key issues involved in developing an appropriate PBD procedure are identified and discussed in the light of the available procedures.

In Sect. 7.3, a PBD procedure is presented based on elastic analysis and the use of the secant stiffness approach and ‘over-damped’ elastic spectra, i.e. the ‘direct displacement based design approach’, pioneered by Priestley and Kowalsky (Priestley et al. 2007; Kowalsky et al. 1995), is extended with a view to making it

applicable to a broad spectrum of bridge systems, including those affected by higher modes, and also introducing additional design criteria not previously used in this method.

In Sect. 7.4 an alternative, more rigorous, method is presented that involves more advanced analysis tools, i.e. response-history analysis (for different levels of ground motion intensity) of bridge models wherein any regions that are expected to yield under the selected seismic actions are modelled as inelastic, whereas the rest of the bridge is modelled as elastic; the initial analysis (relevant to service conditions) is an elastic one. A critical aspect of this (currently under development) procedure is the a-priori definition of the inelastic behaviour of dissipating zones, by exploiting the deformation limits for the specific performance level, which are related to the damage level of the structural members.

Section 7.5 first summarises the current trends worldwide in seismic assessment of bridges and applies the more rigorous assessment procedure, i.e. nonlinear dynamic response-history analysis, to assess the performance of bridges designed to the procedures described in Sects. 7.3 and 7.4. Moreover, comparisons are made between these performance–based designed bridges and similar ones designed to a current international code, namely Eurocode 8.

Finally, in Sect. 7.6, some general conclusions are drawn, regarding the feasibility of using new procedures that aim at a better control of the seismic performance of bridges under different levels of seismic loading.

7.2 Overview of PBD Methods for Bridges

A DDBD procedure was proposed by Kowalsky and his co-workers (Kowalsky 2002; Dwairi and Kowalsky 2006), incorporating basic concepts of the DDBD approach like the target displacement and the displacement profile that should account for inelastic effects, without carrying out an inelastic analysis; the procedure is applicable to multi-degree-of-freedom (MDOF) continuous concrete bridges with flexible or rigid superstructures (decks). A key feature of the method is the EMS (effective mode shape) approach wherein account is taken of higher mode effects by determining the mode shapes of an equivalent elastic model of the bridge based on the column and abutment secant stiffness values at maximum response. A similar version of the method was included in the book by Priestley et al. (2007) on DDBD; this version of the method is simpler than the previously mentioned one (no use of EMS in the design of piers) but also addresses design in the longitudinal direction (which often governs the seismic design of the bridge), and provides some guidance for the treatment of features like the degree of fixity of columns and the effect of higher modes on the superstructure through an EMS approach focusing on forces and moments of the deck only.

Another study (Adhikari et al. 2010) focussed on the difficulties involved in applying DDBD to long-span bridges with tall piers. This study introduced some additional considerations to account for higher mode effects on flexural strength of

plastic hinges in the case of long-span concrete bridges with limited ductile piers. Following the suggestion of Priestley et al. (2007), a response-spectrum analysis (RSA) was used after completion of the DDBD procedure, with two different design spectra (a 5 %-damped design spectrum and a design spectrum with damping value obtained from the DDBD procedure) to determine the design responses (elastic and inelastic, respectively) at critical locations of the bridge as combinations of several modes. The procedure is analogous to what has been called 'Effective Modal Superposition' approach by Priestley and his co-workers (Priestley et al. 2007; Alvarez Botero 2004; Ortiz Restrepo 2006) for bridge design. It is worth noting that in the latter, higher mode effects were considered only for determining the design elastic responses (e.g. deck transverse moment, abutment shear force), whereas inelastic responses, such as flexural strengths at plastic hinge locations, were computed directly from the first inelastic mode, considering that mass participation factor for this mode was always more than 80 %.

The DDBD method was further extended by Suarez and Kowalsky (2007, 2010, 2011) who tackled additional issues such as soil-structure interaction of drilled shaft bents, skewed configurations of piers and/or abutments, conditions under which DDBD can be applied using predefined displacement patterns (including the case of expansion joints), and definition of stability-based target displacements that account for P-Δ effects at the start of the design process. More recently, Kappos et al. (2012a, 2013) have extended the DDBD procedure to properly include higher mode effects and also added additional design criteria (see Sect. 7.3.1).

In an alternative approach, that could qualify as 'indirect' displacement-based design of bridges (Bardakis and Fardis 2011), the concept of calculating inelastic rotation demands from elastic analysis, previously used by Fardis and co-workers for buildings, is extended to concrete bridges having deck integral with the piers.

So far, the vast majority of studies performed on this topic do not consider directly higher mode effects, as a result of the inherent limitation of the procedure (due to the equivalent SDOF approach) to structures wherein the fundamental mode dominates the response.

Some key issues involved in the aforementioned methodologies, which can also serve as a basis for classifying them, are identified and discussed in the remainder of this section.

7.2.1 Type of Analysis

The basic options here are elastic analysis and inelastic analysis, in each case either equivalent static or dynamic. Selection of the type of analysis certainly affects the complexity of the procedure and, up to a certain extent, the time and effort required for carrying out the seismic design of the bridge. It is worth pointing out here that all these methods have been used in at least one of the existing procedures, as discussed in the following.

Equivalent static analysis is the method typically used in the DDBD procedure (Priestley et al. 2007), which starts from a target displacement, consistent with a deformation capacity ensured by an appropriate detailing of the structure. Estimating a reasonable value for the yield displacement, the target displacement translates into a displacement ductility demand and a corresponding equivalent damping ratio, which is used to reduce the selected displacement spectra, to account (indirectly) for nonlinear hysteretic behaviour. Entering this response spectrum with the aforementioned target displacement the effective period (secant value at target displacement) of this system is determined; subsequently, the base shear corresponding to the previously defined peak displacement and the secant stiffness calculated from the effective period, is found. From there on, the procedure reduces to a 'traditional' equivalent lateral force design of the structure. Some empirical corrections for higher modes are suggested in (Priestley et al. 2007).

Elastic dynamic response spectrum analysis is the reference method of current seismic codes in Europe (CEN 2005), the US (Caltrans 2013), and most of the world. These codes can be deemed as performance-based, although in essence they require verification for one performance objective only. The procedure is well known and will not be described herein. Elastic dynamic analysis is also used in PBD methods wherein inelastic rotation demands are estimated from elastic analysis (Bardakis and Fardis 2011).

There is no complete design method that is based on nonlinear static (pushover) analysis, but several methods used for assessment, e.g. the N2 method, have been applied to bridges (Fischinger et al. 2004) and in principle can be applied for DBD adopting a deformation-calculation based approach, i.e. calculation of the expected maximum displacement for an already designed structural system; detailing is then provided such that the displacement capacity of the bridge and its components exceeds the calculated maximum displacement.

Nonlinear dynamic (response-history) analysis is the most rigorous procedure, but also the most difficult to apply. A method proposed by the author and his co-workers is described later (Sect. 7.4) and combines an initial elastic response-history analysis (for determining the strength of dissipating zones, like pier ends) with two sets of nonlinear analyses (two levels of seismic action) wherein displacements and local ductility demands are checked.

7.2.2 Definition of Seismic Input

The definition of the seismic input depends on the type of analysis used, as well as the design approach adopted, i.e.

- Linear dynamic response spectrum analysis requires a design (pseudo-) acceleration spectrum to derive the pertinent modal forces.
- DDBD procedures estimate the required stiffness of the structure through a design displacement spectrum, and then the corresponding base shear as

described previously (Sect. 7.2.1). It is noted here that the long period range of displacement spectra (beyond about 2 s), which is quite important for DDBD that involves secant stiffnesses at maximum displacement, is not yet reliable enough due to the paucity of digital records of ground motion with frequency content rich in this long-period range.

- Response-history analysis requires a set of input accelerograms (at least 7 if average response quantities are to be used for design) which should be compatible with the design spectrum. The critical issue of properly selecting natural accelerograms that are consistent with the design spectrum falls beyond the scope of this chapter; it is only noted that there are currently sound procedures and the associated software, e.g. (Katsanos and Sextos 2013), for selecting 'optimum' sets of seven (or more) accelerograms.

7.2.3 Stiffness of Dissipating Zones

Since displacement control is of paramount importance in all PBD procedures, it is crucial that displacements be not underestimated during the design procedure. In the most common type of bridges, having concrete piers, plastic hinges are typically located at the piers, unless a seismic isolation approach is adopted. The stiffness of the yielding piers is clearly paramount in the calculation of bridge displacements and depends on the level of induced inelasticity (secant stiffness decreases with increasing ductility demand). In this respect, DDBD methods adopt the secant stiffness at maximum displacement approach (effective stiffness taken equal to the ratio of strength to target displacement) and this stiffness is a design parameter, found during the process, as described in Sect. 7.2.1.

Practically all other procedures adopt approximate values of the pier stiffness, corresponding to yield conditions (rather than the max displacement), and this stiffness is assumed as known when design seismic actions (e.g. modal forces) are estimated. For the usual case of reinforced concrete piers, these approximate values are either very rough estimates, like the 0.5 EI_g (50 % of uncracked section rigidity) adopted by both Eurocode 8–1 (CEN 2004) and AASHTO (2010), or slightly more sophisticated ones taking into account the level of axial loading on the pier (which, in general, is not significantly affected by seismic actions) and/or the reinforcement ratio.

Eurocode 8–2 (the Eurocode for Seismic Design of Bridges) (CEN (Comité Europeen de Normalization) 2005) in its (informative) Annex C suggests the following relationship for the effective moment of inertia

$$I_{\text{eff}} = 0.08 I_{\text{g}} + I_{\text{cr}} \tag{7.1}$$

where the cracked section inertia can be calculated as the secant value at yield

$$I_{cr} = M_y / \left(E_c . \varphi_y\right) \tag{7.2}$$

(M_y is the yield moment and φ_y the yield curvature, E_c the concrete modulus). Obviously, I_{cr} can only be estimated from (7.2) when the pier has been designed, so that both strength and yield curvature can be calculated; hence use of the above is feasible only when iterative elastic analyses, or inelastic analysis are used.

The Caltrans Seismic Design Criteria (2013) is a very recently updated document and hence represents the current practice in earthquake-prone areas of the US; importantly, it does not adopt the DDBD procedures that have been developed several years prior to its publication, although it does place particular emphasis on the calculation of displacement demand and capacity. Regarding stiffness, the same concept as in EC8-2 is retained (secant value at yield), the only exception being that the 0.08 I_g term (accounting for tension stiffening effects) is not included in Eq. (7.1). As an alternative, the Caltrans Criteria allow the calculation of effective stiffness as a function of the axial load ratio and the pier reinforcement ratio from graphs provided in (Priestley et al. 1996); this can be directly implemented for carrying out elastic analysis, assuming a reasonable reinforcement ratio and, in principle, analysis should be repeated if the resulting reinforcement is substantially different.

7.2.4 Number of Directly Controlled Design Parameters

Closely related to the issue of pier stiffness, albeit broader, is the issue of the number of directly controlled parameters during the design process. This is arguably the most critical issue, as far as future improvements of seismic design methods for bridges are concerned. Ideally, the designer should both carry out a dimensioning (and reinforcing, in concrete bridges) that satisfies all the selected performance criteria and verify this design by an analysis wherein all member stiffnesses are consistent with the level of inelasticity induced by the seismic actions for which a specific performance objective is verified. This is, clearly, not a realistic design procedure, even if the stiffness and related modelling issues (e.g. gap closures at joints) are overcome by a rather refined nonlinear analysis (accounting for both material and boundary condition nonlinearities). This is, of course, due to the fact that for a reliable nonlinear analysis to be carried out, one needs to know all the details of the bridge, including member dimensions, reinforcement detailing, bearing characteristics, joint widths, and so on. Excluding the case of an epiphany, all these design parameters can at best be guessed at the beginning of the analysis and, as a rule, several iterations will be needed, unless the bridge is overdesigned, rather than designed to meet reasonably closely the selected performance criteria, which would result in an economic design.

In the light of the above, a designer might select to follow the beaten track and use elastic analysis (which is an approximation of the real response of the bridge in

all safety-related verifications) assuming that the period(s) of the structure can be determined beforehand and used to estimate design forces (pseudo-accelerations) that will be used for deriving member action effects (M, V, N) for standard, force-based design. Such a procedure can conveniently account for several factors that affect the seismic response of the bridge, i.e. higher modes, soil-structure interaction, spatial variability of ground motion etc. Nevertheless, satisfaction of the code criteria based on the results of such elastic analyses might well mean simply that the bridge is overdesigned, for instance that smaller piers could have been used without violating any design criteria.

Alternatively, one could select to adopt a DDBD approach, especially during a preliminary design of the bridge (e.g. in the framework of a pre-study), and select as a design parameter the stiffness that has to be assigned to critical members like the piers for the bridge to satisfy the displacement criteria selected as performance indicators. Some of the problems arising from this choice have been discussed in previous sections; it will be added here that target displacements in the DDBD procedure are calculated by empirical procedures, based on assumed inelastic displacement profiles and some calibration studies (Priestley et al. 2007; Kowalsky 2000) that relate pier displacements to material strains (concrete, steel). As a result of the approximations involved, and the fact that material strains and/or local (curvature) ductility requirements are not design parameters, they might end up being different from those envisaged, particularly for bridges with configuration issues.

A tentative conclusion from the above is that a designer should try to strike a balance between the attractive, yet cumbersome if at all feasible, option of directly including several design parameters (member stiffness, displacements, local ductility requirements and/or strain limits), and the more crude approaches like those based on elastic analysis of an assumed as fully known structure, for design forces reduced on the basis of an envisaged global ductility, wherein member forces and displacements are checked at the end of the analysis and if found below the specified limits, the design is assumed to be concluded.

7.2.5 Number of Iterations Required

Last but not least, the practicality of the design procedure also depends on the required number of iterations, in particular the number of required analyses wherein the model of the bridge has to be changed; this, in most cases, requires several sets of analyses run at different times, rather than in a single run, which is the preferred option, especially for practicing engineers. The issue of iterations is closely related to the number of directly controlled design parameters discussed in the previous section. What should be added here is first that for a design approach to be pragmatic the criteria to be satisfied during the iterations should not be excessively strict (e.g. obtaining the target displacement within 1 %), and second that, unfortunately, not all design procedures converge even if the convergence criteria are not

very strict; again this is more the case when higher modes and/or configurations issues are involved (Kappos et al. 2013).

The seismic design procedures described in the next two sections can be deemed as attempts to improve the existing state-of-the-art in PBD of bridges by refining the available procedures; inevitably (in the light of the previous discussions) the proposed improved methods are more cumbersome (to varying degrees) than the existing ones.

7.3 A PBD Procedure Based on Elastic Analysis

For the DDBD method to be applicable to the design for transverse response of bridges with some degree of irregularity, higher mode effects have to be treated as part of the entire design procedure (rather than as a correction of deck shears and moments at the final steps). Hence, in the DDBD method presented in this section the EMS technique (Kowalsky 2002) is included as part of the procedure. A number of idealized bridge configurations were analysed in (Dwairi and Kowalsky 2006) and the results were used for developing guidelines for the selection of displacement patterns (normalized deformed shapes) for continuous bridges with 'rigid translation' and 'flexible symmetric' deformation patterns. These are useful concepts for preliminary design of bridges, but most actual bridges do not fully comply with these idealizations, e.g. the assumption that all columns have the same longitudinal steel ratio and column diameter, or the assumption that piers are hinged to the soffit of the deck, do not hold for many actual bridges. A procedure is then needed that recognises the fact that design codes require taking into account all the peculiarities of each (real) bridge. It is worth recalling here that bridge design documents that are based on the displacement-based concept, such as the AASHTO Guidelines for Seismic Design (AASHTO 2011), require (among other things) the use of nonlinear analysis procedures as part of the design; this inevitably introduces complexity and increases the design effort, especially since the advanced analysis tools have to be used in a number of iterations if over-conservatism is to be avoided. Hence, the initial stimulus for the method presented herein was this very point, i.e. to identify required extensions and/or modifications of the aforementioned DBD procedure, for it to be applicable to actual bridges wherein the simplifying assumptions made at various stages of the procedure (see next section) do not really hold. A further objective was to obtain some preliminary quantitative data regarding the advantages (or otherwise) of applying the DDBD method, compared to 'mainstream' force-based design (FBD), adopted by all current codes.

In view of the aforementioned limitations of DDBD and the fact that bridges are structures wherein higher modes usually play a more critical role than in buildings, the procedure presented herein (Kappos et al. 2013) attempts to refine and extend the procedure for bridges proposed by Dwairi and Kowalsky (2006) by including some additional design criteria and accounting for higher mode effects, not only regarding the proper definition of a target-displacement profile (comprising

non-synchronous displacements, since all significant modes are considered), but also the proper definition of the corresponding peak structural response. The extended procedure, called modal direct displacement-based design, follows the general approach introduced in previous studies of Chopra and Goel (2002) on buildings and Paraskeva et al. (Paraskeva and Kappos 2010; Paraskeva et al. 2006) on bridges, noting that these studies deal with the pushover procedure, rather than with design based on elastic analysis. The efficiency of the presented methodology is then assessed by applying it to an actual bridge, whose different pier heights and the unrestrained transverse displacement at the abutments result in an increased contribution of higher modes. Some additional issues such as the proper consideration of the degree of fixity at the top of the pier and the effect of the deck torsional stiffness are also investigated, and comparisons between the extended and the 'standard' DDBD method are made.

7.3.1 Description of the Procedure

The structure of the method is shown in Fig. 7.1 in flow-chart form; the successive steps are described in the following. Several specific aspects of the method (in particular those related to stiffness values) are applicable to concrete (reinforced and/or prestressed) bridges; however, the basic 'philosophy' of the method is also applicable to steel and composite bridges.

Step 0 – Definition of initial input parameters. General input parameters are defined including geometry, e.g. column height and diameter (in piers with cylindrical columns), mass properties (e.g. translational mass and mass moment of inertia), and material properties. An initial estimate of the column cross-section is required. As a starting point, the output of the dimensioning of the deck and the piers for the Ultimate and Serviceability Limit States under the pertinent combinations of permanent and transient actions can be used. Then, single or multiple performance levels are set as design objectives, by designating the targeted damage states ('damage-based' displacements) for selected seismic hazard levels (expressed in terms of elastic displacement response spectra).

Step 1 – Selection of the displacement pattern. The step prescribed in the 'standard' DDBD procedure (Dwairi and Kowalsky 2006) involves the computation of the relative pier-to-deck stiffness (RS) and the determination of whether the bridge has a rigid or a flexible displacement pattern. Given that the procedure presented here is intended for bridges where higher mode contribution should not be ignored, the flexible displacement pattern scenario is adopted, disregarding the relative stiffness parameter. This means that this step is essentially redundant, nevertheless it is deemed advisable to retain it, as it is always useful for the designer to have a proper indication of the relative stiffness of the deck.

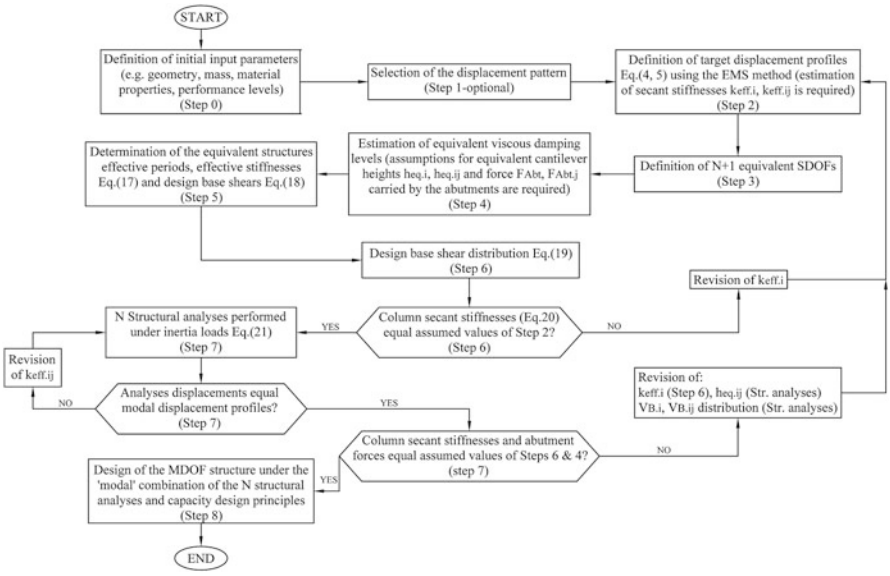

Fig. 7.1 Modal direct displacement-based design of bridges

Step 2 – Definition of target-displacement profiles. The iterative EMS method is followed, according to the following steps:

(i) *Evaluation of mode shapes* ($\boldsymbol{\Phi}_j$): Due to the unavailability of the member effective properties at the beginning of the process, a first estimation is required. Based on current seismic design practice for bridges it can be assumed that the superstructure, particularly in the common case that it is prestressed, will respond essentially elastically, regarding its flexural stiffness, while for the torsional stiffness of prestressed concrete box girders 20 % of the uncracked value can be assumed, based on the ratios ($10 \div 30$ %) of cracked-to-uncracked torsional stiffness estimated by Katsaras et al. (2009). On the other hand, it is suggested that a secant flexural stiffness based on 10 % the gross section rigidity (EI_g) be used for columns expected to deform inelastically, while 60 % EI_g is suggested for columns that are expected to remain below yield. The reduction in the effective axial and shear stiffness (Priestley et al. 1996) of the column(s) can be considered proportional to the reduction in the effective flexural stiffness. Once the structural properties have been established, the eigenvalue problem can be solved, hence the mode shapes $\boldsymbol{\Phi}_j$ can be obtained.

(ii) *Evaluation of modal participation factors* (Γ_j): The modal participation factors can be *computed* using standard procedures, i.e. Eq. (7.3), where $\boldsymbol{m}$ represents a diagonal mass matrix and $\boldsymbol{\iota}$ is a unit vector.

$$\Gamma_j = \frac{\boldsymbol{\Phi}_j{}^T \boldsymbol{mi}}{\boldsymbol{\Phi}_j{}^T \boldsymbol{m} \boldsymbol{\Phi}_j} \tag{7.3}$$

(iii) *Evaluation of peak modal displacements* ($u_{i,j}$): The peak modal displacements are computed according to Eq. (7.4), where index i represents the DOF associated with a lumped mass, as per the inertial discretization, index j represents the mode number, $\Phi_{i,j}$ is the modal factor of joint i at mode j, and S_{dj} is the spectral displacement for mode j obtained by entering the 5 %-damped design spectra with the period obtained from modal analysis.

$$u_{i,\,j} = \Gamma_j \Phi_{i,\,j} S_{d\,j} \tag{7.4}$$

(iv) *Evaluation of expected displacement pattern*: The displacement pattern (δ_i) is obtained by an appropriate combination of the peak modal displacements, such as the SRSS combination given by Eq. (7.5); CQC combination is expected to yield better results when the natural frequencies of the participating modes in the response are closely spaced.

$$\delta_i = \sqrt{\sum_j u^2{}_{i,\,j}} \tag{7.5}$$

It is noted that a displacement pattern derived from the above procedure accounts for the effect of all significant modes (e.g. those needed to capture around 90 % of the total mass in the transverse direction); therefore, it does not correspond to an actual inelastic deformed shape of the bridge, particularly so in the case of asymmetric systems. To obtain the target displacement profile (Δ_i), the displacement pattern given by Eq. (7.5) is scaled in such a way that none of the member (pier or abutment) displacements exceeds the target displacements obtained based on strain or drift criteria:

$$\Delta_i = \delta_i \frac{\Delta_{D,c}}{\delta_c} \tag{7.6}$$

where $\Delta_{D,c}$ and δ_c are the 'damage-based' displacement and the modal value at the location of the critical member, c, whose displacement governs the design, respectively. Prior to applying (7.6) one iteration might be needed to identify the most critical member, when this is not obvious. Then, peak modal displacements ($u_{i,j}$) are scaled to N modal target-displacement profiles ($U_{i,j}$) using the same scaling coefficient as that used to obtain the target-displacement profile in Eq. (7.6):

$$U_{i,\,j} = u_{i,\,j} \frac{\Delta_{D,\,c}}{\delta_c} \tag{7.7}$$

An immediate consequence of the aforementioned procedure is that the combination of the N modal target-displacement profiles ($U_{i,j}$) yields the target-displacement profile (Δ_i); hence, when the SRSS combination rule is used:

$$\Delta_i = \sqrt{\sum_j U^2{}_{i,\,j}} \tag{7.8}$$

Step 3 – Definition of N + 1 equivalent SDOF structures. These idealised structures are established based on equality of the work done by the MDOF bridge and the equivalent SDOF structure (Calvi and Kingsley 1995). Each of the N SDOF structures is related to the corresponding modal target-displacement profile ($U_{i,j}$), whereas the additional SDOF is related to the (final) target-displacement profile (Δ_i). Utilizing Eqs. (7.9) and (7.10), an equivalent system displacement (Δ_{sys}, $U_{sys,j}$), mass (M_{sys}, $M_{sys,j}$), and location (x_{sys}, $x_{sys,j}$) of the SDOF across the MDOF bridge deck is computed for each of the $N+1$ SDOF structures; the 'location' of the SDOF system (i.e. of the masses M_{sys} *or* $M_{sys,j}$) coincides with the point at which the resultant of the modal forces is applied, and is one of the criteria used for checking convergence of the procedure. In Eqs. (7.9) and (7.10), m_i is the mass associated with joint i, and n is the number of joints as per the inertial discretization.

$$U_{sys,\,j} = \frac{\sum_{i=1}^{n} m_i U_{i,\,j}{}^2}{\sum_{i=1}^{n} m_i U_{i,\,j}}, \quad M_{sys(j)} = \frac{\sum_{i=1}^{n} m_i U_{i,\,j}}{U_{sys,\,j}}, \quad x_{sys,\,j} = \frac{\sum_{i=1}^{n} \left(m_i U_{i,\,j} x_i\right)}{\sum_{i=1}^{n} \left(m_i U_{i,\,j}\right)} \tag{7.9}$$

$$\Delta_{sys} = \frac{\sum_{i=1}^{n} m_i \Delta_i{}^2}{\sum_{i=1}^{n} m_i \Delta_i}, \quad M_{sys} = \frac{\sum_{i=1}^{n} m_i \Delta_i}{\Delta_{sys}}, \quad x_{sys} = \frac{\sum_{i=1}^{n} \left(m_i \Delta_i x_i\right)}{\sum_{i=1}^{n} \left(m_i \Delta_i\right)} \tag{7.10}$$

Step 4 – Estimation of equivalent viscous damping levels. Utilizing the target displacement (Δ_i) and the modal target-displacement profiles ($U_{i,j}$), the ductility level is calculated for each member (for each of the $N+1$ profiles), according to Eq. (7.11). Yield curvatures are estimated using Eq. (7.12), where ε_y is the reinforcement yield strain and D is the diameter of a circular section; similar equations are provided for different section shapes (Priestley et al. 1996, 2007).

$$\mu_{\Delta_i} = \Delta_i / \Delta_{yi}, \quad \left(or\ \mu_{\Delta_i} = U_{i,\,j} / \Delta_{yi,\,j}\right) \tag{7.11}$$

$$\varphi_y = 2.25 \varepsilon_y / D \tag{7.12}$$

Figure 7.2 shows the modelling of a pier with a rigid base, whose top is monolithically connected to the deck, whereas possible moment diagrams under transverse loading are also illustrated. A pier moment diagram consists of two

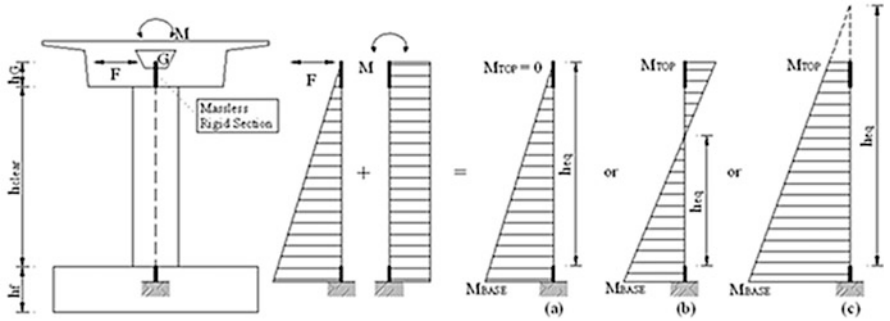

Fig. 7.2 Pier modelling and transverse response accounting for the torsional stiffness of the deck; inflection point: (**a**) at the top; (**b**) inside the pier; (**c**) above the pier

different components; the bending moment derived from the inertial horizontal forces F, acting on the mass centroid (G), and the bending moment induced from the eccentricity of the latter forces with respect to the shear centre, in the usual case wherein the shear centre does not coincide with the mass centroid. The final moment diagram depends on the cracked torsional stiffness of the bridge deck, the superstructure-abutment connection and the pier-superstructure relative stiffness. Likewise it is required to properly account for the degree of fixity at the pier top and hence for the transverse response of the pier regarding its flexural stiffness (k_{pier}) and yield displacement ($\Delta_{y,pier}$), according to Eqs. (7.13) and (7.14a, 7.14b), (referring to case (b) in Fig. 7.2; similar relationships apply to the other cases).

$$x_k = \frac{h_{eq}}{h} = \frac{h_{eq}}{h_{clear}+h_G}, \quad k_{eq} = \frac{3EI}{h_{eq}^{\,3}}, \quad k_{pier} = x_k k_{eq} \tag{7.13}$$

$$x_{\Delta y} = \frac{L_{eq}}{L_{eff}} = \frac{h_{eq}+0.022 f_y d_{bl}}{h_{clear}+h_G+0.022 f_y d_{bl}} \tag{7.14a}$$

$$\Delta_{y,\,eq} = \frac{\varphi_y L_{eq}^{\,2}}{3}, \quad \Delta_{y,\,pier} = \frac{1}{x_{\Delta y}}\Delta_{y,\,eq} \tag{7.14b}$$

In Eqs. (7.13) and (7.14a, 7.14b), $\Delta_{y,eq.}$ and k_{eq} are the yield displacement and the flexural stiffness of the equivalent cantilever, E is the elastic modulus of the pier material, I is the moment of inertia of the pier cross-section (modified for cracking effects wherever necessary), d_{bl} is the longitudinal reinforcement bar diameter and $0.022\ f_y d_{bl}$ is the strain penetration length (where f_y is the yield stress of the longitudinal reinforcement in MPA). The height of the equivalent cantilever (h_{eq}) cannot be determined at the initial stage of design, therefore either preliminary structural analyses should be performed for each of the $N+1$ equivalent structures under lateral loads compatible with the corresponding profile, or an assumption that the height of the equivalent cantilever equals the height of the pier, be made during the first iteration. The first approach is strongly recommended for the case of

significant higher mode effects, since it reduces the number of iterations required to achieve convergence.

Several relationships (Blandon and Priestley 2005; Guyader and Iwan 2006; Dwairi et al. 2007) between hysteretic damping and ductility have been proposed. The one proposed in (Dwairi et al. 2007) based on Takeda's hysteretic model (Takeda et al. 1970), given by Eq. (7.15), is used herein. Additional elastic viscous damping (ξ_v) up to 5 % should be added to the hysteretic damping in line with the approach proposed by Grant et al. (Grant et al. 2004).

$$\xi_i = \xi_v + \frac{50}{\pi}\left(\frac{\mu_\Delta - 1}{\mu_\Delta}\right)\% \tag{7.15}$$

These damping values need to be combined in some form to obtain system damping for each of the $N+1$ equivalent SDOF structures. A weighted average can be computed, as given by Eq. (7.16), where $W_i/\Sigma W_k$ is a weighting factor, based on the work (W_i) done by each member (Eq. (7.17)), according to (Kowalsky 2002)

$$\xi_{sys} = \sum_{i=1}^{n}\left(\frac{W_i}{\sum_{k=1}^{n} W_k}\xi_i\right), \quad \xi_{sys(j)} = \sum_{i=1}^{n}\left(\frac{W_{i,j}}{\sum_{k=1}^{n} W_{k,j}}\xi_{i,j}\right) \tag{7.16}$$

$$W_i = V_i\Delta_i, \quad W_{i,j} = V_{i,j}U_{i,j} \tag{7.17}$$

Calculation of the weighting factors presupposes knowledge of member forces (V_i), which are not known at the current step. As a starting point, it can be assumed that the seismic force carried by the abutments is equal to 30 % of the total seismic force carried by the bridge and column shears are inversely proportional to column heights, as illustrated by Eq. (7.18) (Kowalsky 2002), where μ is less than one for elastic columns and equal to one for columns that have yielded. In subsequent iterations, system damping is computed using member forces obtained from structural analysis.

$$W_i = \mu_{\Delta_i}\Delta_i/h_{eq,i}, \quad W_{i,j} = \mu_{\Delta_i}U_{i,j}/h_{eq,ij} \tag{7.18}$$

Step 5 – Determination of the effective periods of the equivalent structures. Utilizing the $N+1$ system target displacements (Δ_{sys}, $U_{sys,j}$), levels of system damping (ξ_{sys}, $\xi_{sys,j}$), and elastic response spectra for the chosen seismic demand, the effective periods (T_{eff}, $T_{eff,j}$) of the equivalent structures are determined from the design spectrum (see next section). Once the effective periods have been determined, effective stiffnesses (k_{eff}, $k_{eff,j}$) and design base shears (V_B, $V_{B,j}$) are computed by Eqs. (7.19) and (7.20), respectively.

$$k_{eff} = 4\pi^2 M_{sys}/{T_{eff}}^2, \quad k_{eff,\,j} = 4\pi^2 M_{sys,\,j}/{T_{eff,\,j}}^2 \tag{7.19}$$

$$V_B = k_{eff}\Delta_{sys}, \quad V_{B,\,j} = k_{eff,\,j}U_{sys,\,j} \tag{7.20}$$

Step 6 – Verification of design assumptions. Design base shears (V_B, $V_{B,j}$) are distributed in proportion to the inverse of the column height according to Eq. (7.21), which is based on the simplifying assumption that all columns have the same diameter and longitudinal reinforcement ratio, zero post-elastic slope of the force-displacement response, mass small enough, so that inertia forces due to self-weight can be neglected, and the same end-fixity conditions. In Eq. (7.21) μ_i and μ_k are less than one for elastic columns and equal to one for columns that have yielded, and F_{Abt} represents the total force carried by the abutments. R/C member cracked section stiffnesses are computed for each of the $N+1$ profiles, using Eq. (7.22) and are compared with values assumed at Step 2. If the values related to the target-displacement profile (Δ_i) differ significantly, computed secant stiffnesses ($k_{eff,i}$) are utilized in the EMS to obtain revised target-displacement profiles (Δ_i, $U_{i,j}$). Steps 2–6 are repeated by changing column secant stiffnesses until the target profile (Δ_i) stabilises. Although a strict approach requires iteration within Steps 2–6 until all profiles (Δ_i and $U_{i,j}$) stabilise, the implementation of the methodology in the next section indicates that whenever Δ_i stabilises, $U_{i,j}$ also practically stabilise, hence Δ_i can be used as the sole convergence criterion.

$$V_{B,k} = (V_B - F_{Abt})\frac{\mu_{\Delta,k}}{h_k}/\sum_{i=1}^{n}\frac{\mu_{\Delta,i}}{h_i}, \quad V_{B,kj} = \left(V_{B,\,j} - F_{Abt,\,j}\right)\frac{\mu_{\Delta,kj}}{h_k}/\sum_{i=1}^{n}\frac{\mu_{\Delta,ij}}{h_i} \tag{7.21}$$

$$k_{eff,\,i} = V_{B,i}/\Delta_i, \quad k_{eff,\,ij} = V_{B,ij}/U_{i,\,j} \tag{7.22}$$

Step 7 – Structural analysis. Once the target-displacement profile (Δ_i) stabilises, base shears ($V_{B,j}$) are distributed as inertia forces to the masses of the MDOF structure in accordance with the modal target-displacement profiles ($U_{i,j}$), given by Eq. (7.23) (Calvi and Kingsley 1995). In this equation $F_{i,j}$ are the bent inertia forces, $V_{B,j}$ are the design base shears, indices i and k refer to joint numbers, and n is the number of joints.

$$F_{k,\,j} = V_{B,\,j}\left(m_k U_{i,\,j}\right)/\sum_{i=1}^{n}\left(m_i U_{i,\,j}\right) \tag{7.23}$$

N structural analyses (as many as the significant modes) are performed on the bridge under the inertia loads, to obtain the 'modal' base shear for each column. Secant stiffnesses $k_{eff,ij}$ obtained from the iteration within Step 6, at which stabilisation of Δ_i (hence stabilisation of $U_{i,j}$ as mentioned in Step 6) was observed, should be used in each of the N structural analyses, in order to be consistent with the DDBD philosophy. Afterwards, displacements derived from the N structural analyses are compared with the corresponding profiles $U_{i,j}$. In the case of significantly different displacements, reasonable values for column secant stiffnesses are

assumed and analyses are conducted until convergence is achieved. Once the displacement profiles obtained from structural analyses converge to the assumed modal target-displacement profiles, column secant stiffnesses and abutment forces from each analysis are compared with the values assumed at Step 6, at which stabilisation of $U_{i,j}$ was achieved. It is reminded that during the first loop of iterations the seismic force carried by the abutments is assumed equal to 30 % of the total seismic force carried by the bridge for all the $N+1$ cases. In case of significant discrepancy, the target-displacement profile is revised utilising the EMS method and forces from structural analysis. Steps 2–7 are repeated, until column secant stiffnesses and abutment forces converge.

In order to perform the new loop of iterations and the new EMS in particular, previous loop secant stiffnesses ($k_{eff,i}$) (Step 6) can be assumed as the starting point. Furthermore, revised equivalent cantilever heights are computed according to the results of the N structural analyses, which were previously performed, as far as the modal target-displacement profiles ($U_{i,j}$) are concerned, whereas in the case of the (final) target-displacement profile (Δ_i), proper values of the equivalent cantilever heights can be approximately determined by combining the peak 'modal' responses (N structural analyses). Following the same approach, the force carried by the abutments and the base shear distribution for each of the $N+1$ cases required in the subsequent steps are determined from analysis results, instead of utilising Eq. (7.21), which, given the diversity of the column end-fixity conditions, is not accurate enough.

Step 8 – Design of the MDOF structure The MDOF bridge is designed in accordance with capacity design principles (e.g. (CEN 2005; Priestley et al. 1996)) such that the desired failure mechanism is achieved. The response quantities of design interest (displacements, plastic hinge rotations, internal pier forces) are determined by combining the peak 'modal' responses (from the N structural analyses), using an appropriate modal combination rule (e.g. SRSS or CQC), and superimposing the pertinent combinations of permanent and transient actions.

7.3.2 Application of the Procedure

The various steps of the PBD method described in Sect. 7.3.1 are applied in the following to an actual concrete bridge (Kappos et al. 2013), whose different pier heights and the unrestrained transverse displacement at the abutments result in an increased contribution of the second mode. The bridge is designed both to the 'standard' DDBD procedure proposed by Kowalsky and co-workers (Kowalsky 2002; Dwairi and Kowalsky 2006) and to the more rigorous procedure described in Sect. 7.3.1.

7.3.2.1 Description of Studied Bridge

The selected structure (Overpass T7 in Egnatia Motorway, N. Greece), is quite common in modern motorway construction in Europe. The 3-span structure of total length equal to 99 m (see Fig. 7.3) is characterized by a significant longitudinal slope (approximately 7 %). The deck consists of a 10 m wide prestressed concrete box girder section with a variable geometry across the longitudinal axis of the bridge (see Fig. 7.3). The two piers have a cylindrical cross section, and unequal height (clear column height of 5.94 and 7.93 m), due to the deck's longitudinal inclination. The deck is monolithically connected to the two piers, while it rests on its abutments through elastomeric bearings; movement in both the longitudinal and the transverse direction is initially allowed at the abutments, but transverse displacements are restrained in the actual bridge whenever the 15 cm gap shown at the bottom of Fig. 7.3 is closed. In applying the proposed design procedure to this bridge, the gap size, as well as the characteristics of the bearings are treated as design parameters. The bridge rests on firm soil and the piers and abutments are supported on surface foundations (footings) of similar configuration.

The T7 Overpass was redesigned (Kappos et al. 2013) using DDBD, both in the form proposed in (Dwairi and Kowalsky 2006), and its modified version presented herein, for two different seismic zones. The Greek Seismic Code (EAK 2000) elastic spectrum (Ministry of Public Works of Greece 2010) for Zone II (PGA of 0.24 g) and III (PGA of 0.36 g) was the basis for seismic design; it corresponded to ground conditions category 'B' of the Code, which can be deemed equivalent to subsoil class 'B' of older drafts of Eurocode 8 and closer to ground 'C' in its final

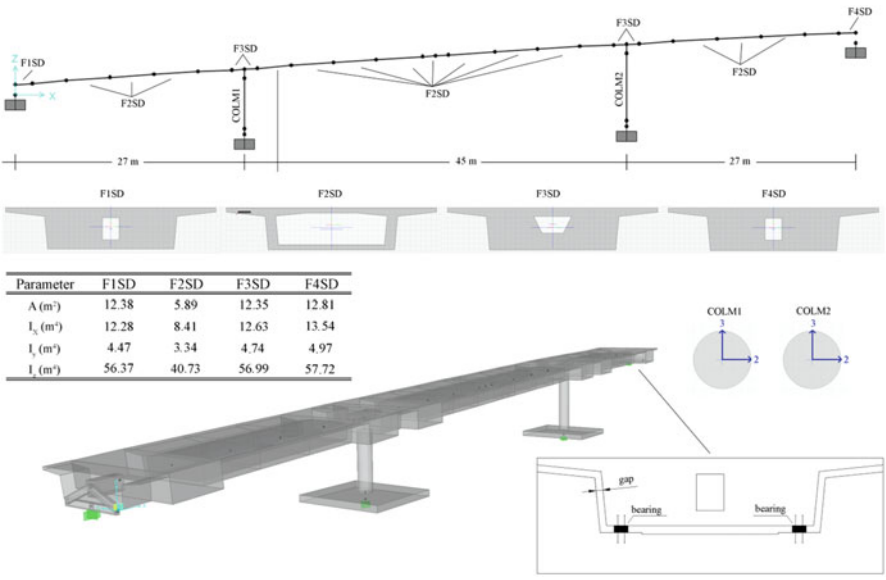

Fig. 7.3 Layout of the bridge configuration and finite element modelling

version (CEN 2004). The bridge was designed as a ductile structure, implying that plastic hinges are expected to form in the piers, while P-Δ effects were taken into consideration. A further parameter that was investigated in applying the DDBD was the effect of the girder torsional stiffness.

In the analyses presented in the following, the focus is on the transverse response of the bridge, as it is well known that this is the most affected by higher modes. Additional analyses in the longitudinal direction were also conducted, however due to space limitations and the fact that longitudinal design was found to be less critical, these analyses are not presented herein. The analysis was carried out using the Ruaumoko 3D software (Carr 2006), whereas SAP2000 (CSI [Computers and Structures Inc.] 2007) was also used for additional verification; the reference finite element model (Fig. 7.3) involved 32 non-prismatic 3D beam-column elements. The elastomeric bearings present at the abutments were modelled using equivalent linear springs ('Link elements' in SAP2000, 'Spring type members' in Ruaumoko) with six DOFs.

Preliminary analyses accounting for soil-structure interaction (SSI) effects, using a foundation compliance matrix, have shown that due to the relatively stiff soil formations underneath the studied bridge, SSI had little effect on the response; hence these effects were subsequently ignored in the design of the bridge.

7.3.2.2 'Standard' Direct Displacement-Based Design (DDBD)

A 'standard' DDBD (Kowalsky 2002; Dwairi and Kowalsky 2006) was first performed, mainly to identify the limitations of the procedure, which arise from its inherent restriction to structures wherein the fundamental mode dominates the response (Calvi and Kingsley 1995). As shown later, the transverse response of the overpass is determined by two dominant modes. A 'damage control' limit state that corresponds to a drift ratio of 3 % was considered; qualitatively, 'damage control' implies that only repairable damage occurs in the columns.

The design displacement spectrum (Fig. 7.4) was derived from the pertinent elastic acceleration response spectrum ($S_d = S_a/\omega^2$). A significant modification was made to the spectrum used for design, i.e. the corner period in S_d was taken equal to 4.0 s, according to the SEAOC (Ad Hoc Committee 1999) recommendations, which is substantially longer than the period values of 2.0 and 2.5 specified by EC8 and the National Annex of Greece, respectively. This modification is not only in line with recent research findings, but also necessary for DDBD to be meaningful (Kappos 2010), in the sense that short corner periods lead to small displacement values in the period range that is common to DDBD (up to the linear branch), which involves secant stiffness values at maximum displacement.

Moreover, the modification to the elastic acceleration spectrum, required to account for ductile response through an increased effective damping ratio, was made using the damping modifier (η) adopted in the final version of EC8 (CEN 2004), i.e. Eq. (7.24) below, where ξ_{sys} is the viscous damping ratio of the structure, expressed as a percentage.

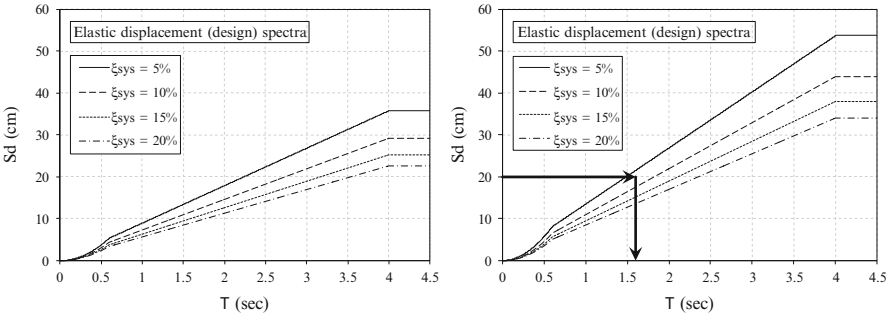

Fig. 7.4 Elastic displacement response spectra for various damping ratios; *left*: Zone II (PGA = 0.24 g), *right*: Zone III (PGA = 0.36 g)

$$\eta = \sqrt{10/\left(5+\xi_{sys}\right)} \tag{7.24}$$

As previously mentioned, the mechanical characteristics of the elastomeric bearings are a design parameter since they affect the displacement capacity of the bridge; hence an initial estimate is required. A rational choice of the elastomer cross-sectional area can be made on the basis of the axial load resulting from service loading, while the total thickness (t_r) of the elastomer should provide the target-displacement profile (see Fig. 7.5) with adequate displacements at the abutments, so that the 'damage-based' displacements (Δ_D) of each column, related to the acceptable drift ratio, could be attained, and a reasonable longitudinal reinforcement ratio could be obtained for the columns. The elastomeric bearings selected herein are rectangular in shape (350 mm × 450 mm) with t_r of 88 mm, horizontal stiffness of 2,506 kN/m and equivalent viscous damping ratio equal to 5 %; two bearings are placed on each abutment, as shown in Fig. 7.3 (bottom-right). The maximum acceptable shear strain ratio (γ_u), from which the 'damage-based' displacements of the bearings are derived, is taken equal to 2.0. Introducing the 3 % drift ratios for the columns and accounting for strain penetration effects, the 'damage-based' displacements of all members (piers or abutments) were defined as $\Delta_{D,Abt} = 0.176$, $\Delta_{D,Col1} = 0.218$, $\Delta_{D,Col2} = 0.278$ m; a diameter of 2.0 m was initially assumed for the two columns (as in the original design of the bridge).

To obtain the target-displacement profile for the inelastic system, the EMS method (Kowalsky 2002) is used. It is assumed that the prestressed deck will respond essentially elastically, as far as its flexural stiffness is concerned, while its torsional stiffness is set equal to 20 % of the uncracked section torsional stiffness. A secant flexural stiffness equal to 10 % the gross value is applied to the columns (both of them are expected to respond inelastically), while the reduction in the effective axial and shear stiffness is considered to be proportional to the reduction in flexural stiffness. Figure 7.5 illustrates the target-displacement profiles derived from applying the EMS method iteratively; displacement patterns, peak modal displacements and modal mass participation factors for each mode are also

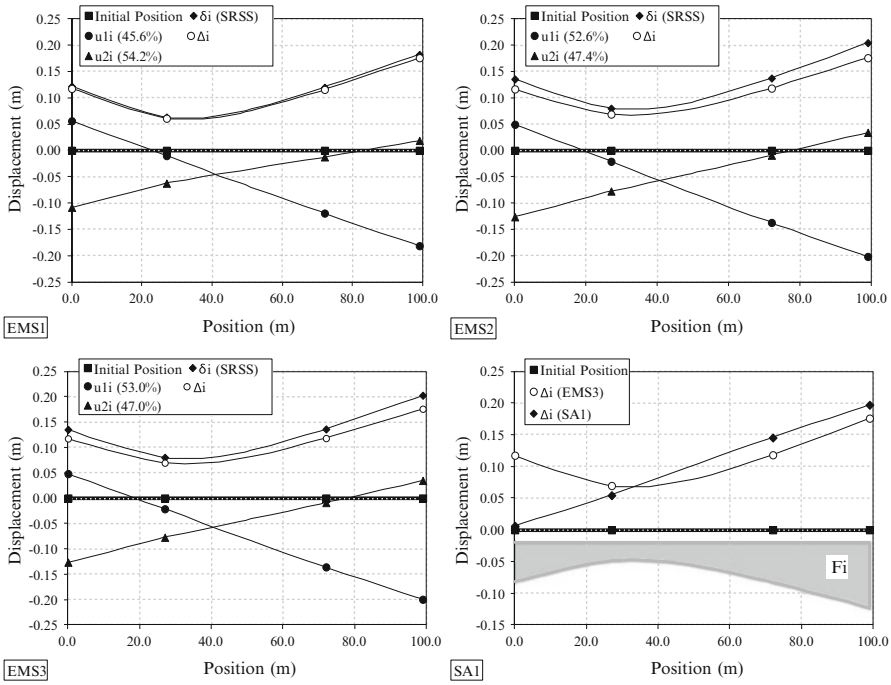

Fig. 7.5 Displacement profiles (EMS): Peak modal displacements $u_{i,j}$, displacement pattern δ_i and target-displacement profiles Δ_i, estimated iteratively from the EMS method. Structural analysis displacement profile (SA1) compared with target-displacement profile (inertia forces (F_i) on the MDOF structure also illustrated)

shown. Convergence was checked with regard to stabilisation of the target-displacement profile or the column secant stiffness from one iteration to the next. Dots on the graphs represent the points of the deck axis passing through its mass centroid, corresponding to the centres of elastomeric bearings and columns.

The next step of the 'standard' DDBD method involves structural analysis of the bridge under the inertia loads given by Eq. (7.23), (where, in the 'standard' procedure, $U_{i,j}$ corresponds to Δ_i), to obtain the design shear at the base of each column. In Fig. 7.5 (bottom-right) the displacement profile derived from structural analysis Δ_i (SA1), is compared with the target-displacement profile Δ_i (denoted as EMS3). The discrepancy between the two profiles reveals one of the main deficiencies of the 'standard' DDBD, i.e. its inability to predict the peak structural response (in terms of displacements and hence internal member forces), on the basis of which design will be carried out.

The target-displacement profile, which generally reflects the ultimate limit state (in terms of displacements) of the structural members, was constructed from the combination of the peak modal displacements (according to the SRSS rule), and then scaled in such a way that none of the member displacements exceeded the 'damage-based' design values. By following this procedure, the target-

displacement profile never reflects an actual deformed shape of the structure; instead, it represents a fictitious deformed shape comprised of non-simultaneous displacements, which is deemed to reflect the peak (and non-simultaneous) structural member response. Therefore, in cases (like here) where more than one modes dominate the response, a static structural analysis under a modal combination of seismic lateral forces such as those given by Eq. (7.23) (whose distribution is also shown in Fig. 7.5, bottom-right), cannot, under any circumstances, produce the target-displacement profile. The above discrepancy in the displacement profiles is due neither to errors in the estimation of the equivalent cantilever heights nor to the approximate base shear distribution according to Eq. (7.21) (Kappos et al. 2013).

To be able to compare results from the existing DDBD method with those of the proposed one, the requirement of convergence of the entire profiles was replaced by a lower requirement, namely convergence at the locations of two supporting members only, first the Abutment 2 (that has the largest displacement) and Column 2 (that is the one closest to Abutment 2), and then (as an alternative) the two columns, although neither exhibits the largest design displacement. As shown in Fig. 7.6, several iterations (adjustments of member effective stiffness) using the converged profile from EMS ('Loop 1-Δi(EMS3) in the figure) fail to obtain even a rough match between the EMS displacement profile and that obtained from structural analysis (Δi(SA) in the figure) on the left part of the bridge, while convergence is reached in the area of the left column and the left abutment (Abt2), which are affected by the fundamental mode of the bridge (see also Figs. 7.5 and 7.7). As a result of this, the design of Abutment 1 and Column 1 on the basis of the aforementioned structural analysis is not correct. Similar comments apply in the other case studied, wherein convergence was sought for the two columns.

7.3.2.3 Modal Direct Displacement-Based Design (MDDBD)

The extended (modal) DDBD procedure described in Sect. 7.3.1 was applied to the previous case study; more details than those given herein can be found in (Kappos et al. 2013) and its Appendix available on line.

As in the 'standard' DDBD, a 2.0 m column diameter was assumed as a starting point. However, seismic design for Zone II resulted in column longitudinal reinforcement ratios less than the minimum required by bridge codes. Due to the fact that providing the minimum required ratio would obscure the concepts of DDBD (regarding the target profile, displacement ductilities etc.) and aiming at an optimum design, a 1.5 m column diameter was subsequently used. Preliminary structural analyses were performed for each of the three equivalent SDOF systems (N + 1, considering the first 2 modes), under lateral loads compatible with the modal profiles and their SRSS combination, to obtain the equivalent cantilever heights and the uncracked stiffnesses ($K_{g,i}$), according to Eq. (7.13). The assumed characteristics of the elastomeric bearings, the design spectrum and the 'damage-based' displacements were determined as in the 'standard' DDBD.

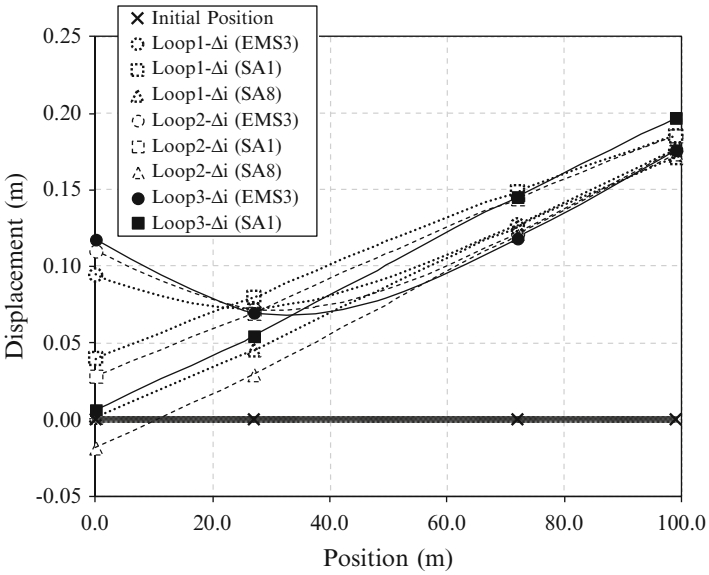

Fig. 7.6 Target-displacement profiles Δi(EMS), structural analysis displacement profiles (SA1) based on the secant stiffnesses of EMS and revised structural analysis displacement profiles (SA) that converge to the target-displacement of the critical member (i.e. Abt2) and Col2, derived iteratively from the DDBD methodology

To establish the initial displacement profiles, a modal analysis was conducted where member stiffnesses were set as in the 'standard' DDBD. The peak modal displacements ($u_{i,j}$), the displacement pattern (δ_i), the target-displacement profile (Δ_i) and the modal target displacement profiles ($U_{i,j}$) are shown in Fig. 7.7, and it is clear that the abutments are the critical elements. The three equivalent SDOF systems were defined in accordance with Eqs. (7.9) and (7.10).

Once the target-displacement profiles were established, the individual member ductility values (Eqs. (7.11)) were calculated along with the corresponding equivalent viscous damping values (Eq. (7.15)), where elastomeric bearings were assumed to respond elastically ($\xi_{Abt} = 5\,\%$). Assuming that 30 % of the total shear is carried by the abutments (in all 3 cases), the equivalent system damping values were obtained. The effective periods at maximum response were then obtained from the displacement spectra (Fig. 7.4) and then the secant stiffnesses at maximum response were determined. Design base shears were calculated from Eq. (7.20) and member shear forces from Eq. (7.21). As soon as base shears for the SDOF systems are defined, the fraction of the shear carried by the abutments can be recalculated. If the revised fractions of the base shear differ significantly from the assumed values (30 %), Steps 4 and 5 are repeated until fractions of x_{Abt} stabilise. It is clear than in the common case of seat-type abutments with bearings the design is simplified on the grounds that the shear carried by the abutment is known from the first iteration. The column secant stiffness values can be recalculated at this point since column

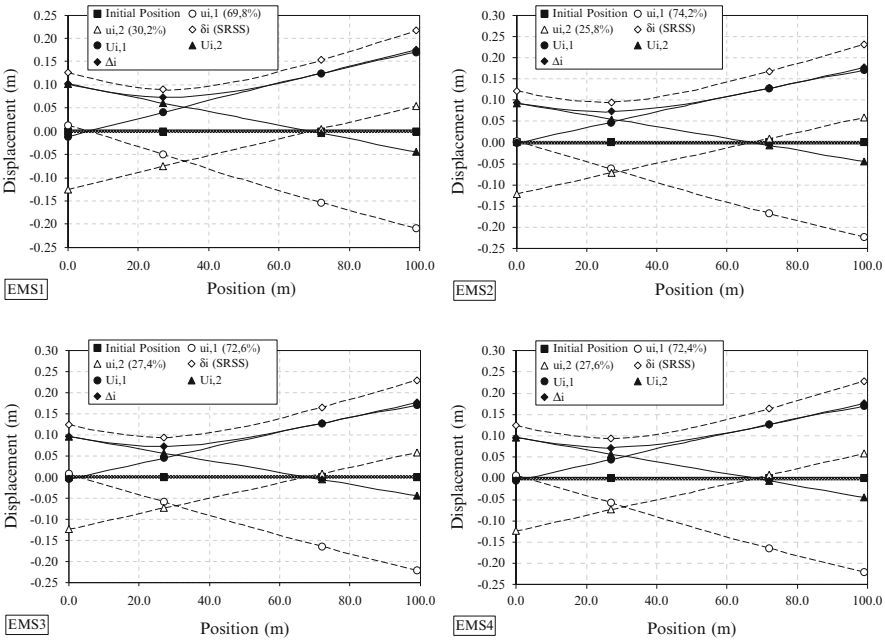

Fig. 7.7 Displacement profiles: Peak modal displacements ui,j, displacement pattern δi, modal target-displacement profiles Ui,j and target-displacement profiles Δi, derived iteratively from the EMS method

forces and member displacements are now known. This is then followed by a revised modal analysis with the new secant stiffness properties resulting into new target-displacement profiles (Δ_i, U_{ij}). In total, four iterations were needed until Δ_i stabilised. The finally derived profiles are illustrated in Fig. 7.7. It is evident (from Iterations 3 and 4), that whenever Δ_i stabilises, $U_{i,j}$ also stabilise.

Once the target-displacement profile (Δ_i) converged, two structural analyses of the MDOF structure were performed under the inertia forces of Eq. (7.21), using the secant stiffnesses from the 4th Iteration (Mode 1 and Mode 2). Due to the inconsistency of the derived displacements ($U_{an,ij}$) with the corresponding modal target displacements ($U_{i,j}$), the two analyses were repeated with revised secant stiffnesses until convergence was achieved; U_{i1} and U_{i2} converged after 8 and 5 iterations, respectively. The shear carried by the abutments in the last iteration closely matches the values obtained through EMS (Iteration 4), due to the fact that bearing stiffness is assumed constant, determined from the initial selection of the bearing characteristics. Since the final secant stiffnesses of the columns differed significantly from the assumed ones (Kappos et al. 2013), Steps 1 to 7 were repeated, and new equivalent cantilever heights and column shear distribution were defined from the analysis.

The new loop of iterations attempts to reduce the discrepancy resulting from updating the equivalent cantilever height (which does not change much with respect

to the initially assumed value), and the shear distribution effect according to Eq. (7.21), but not the fraction of the shear carried by the abutments, since this is considered known, as already discussed. It is noted that the $\Delta_{an,i}$ is derived from the SRSS combination of $U_{an,ij}$.

The response quantities of design interest (rotations, internal pier forces) are determined by combining the peak 'modal' responses (from the two structural analyses), using the SRSS combination rule, superimposed with the pertinent combinations of permanent and transient actions. P-Δ effects were also taken into account, and it was verified that the stability index satisfied $\theta_\Delta \leq 0.20$. Finally, the design procedure yielded a longitudinal steel ratio of 9.8‰ and 12.4‰ for Col_1 and Col_2, respectively. The ratio of Col_1 is just slightly less than the minimum required ratio (1 %), according to the Eurocode.

The procedure was repeated for the case of Zone III (see Fig. 7.4) in which case a 2.0 m column diameter was selected. In this case the design yielded a longitudinal steel ratio of 11.5 and 19.0‰ for Col_1 and Col_2, respectively.

An additional investigation regarding the effect of the box girder torsional stiffness throughout the suggested methodology can be found in (Fischinger et al. 2004). It was found that while a zero torsional stiffness assumption simplifies the design procedure (no iteration for the equivalent cantilever heights is required), it also overestimates the required longitudinal steel ratios (4.2 and 6.2 % for Col_1 and Col_2, respectively) and hence leads to uneconomical design.

7.4 A PBD Procedure Based on Inelastic Analysis

The PBD procedure based on deformation control and involving inelastic response-history analysis, proposed for buildings by Kappos and Stefanidou (2010) is tailored herein to seismic design of bridges. It will be seen that several modifications are required, primarily arising from the fact that the favourable plastic mechanism is different in bridges (energy dissipation takes place in the vertical members, i.e. the piers). Although reference to response-history analysis is made throughout, it should be understood that nonlinear static procedures that duly account for higher mode effects (see Sect. 7.5) can also be used in many cases.

7.4.1 Description of the Procedure

Step 1 – Flexural design of plastic hinge zones based on operationality criteria. The purpose of this step is to establish a basic level of strength in the structure that would ensure that the bridge remains operational during and after an earthquake having a high probability of exceedance (usually taken as 50 % in 50 years). The operationality verifications include specific limits for member ductility factors and plastic hinge rotations of critical members (see Step 4) and the corresponding

demands are estimated from *inelastic* analysis of a partially inelastic model of the structure (described in Step 3). Since for any inelastic analysis to be carried out the strength of the yielding zones must be an input parameter, an *initial* elastic analysis is required, which would provide the strength of the members (energy dissipation zones) that will respond inelastically during the operationality verification; this analysis constitutes Step 1 and is a vital part of the procedure.

The design of selected dissipation zones, like the pier ends, is carried out using conventional elastic analysis (modal response spectrum, or equivalent static, analysis, depending on the structural system). The strength of these zones is estimated taking into consideration the range within which the inelastic deformations should fall, which corresponds to the degree of damage allowed for the selected performance level (more specifically the allowable rotational ductility factor). The procedure described in the following leads to attaining the permissible values of inelastic deformations (expressed through ductility factors), since the latter are directly related to the reduction of element forces corresponding to elastic behaviour. This is a critical feature, not included in earlier versions of the method (tailored to buildings) that simply included a serviceability check, the result of which typically was that most members either remained elastic or were well below the allowable deformation limits (Kappos and Panagopoulos 2004). The design procedure described herein aims at the development of the selected inelastic deformations in the piers, directly using rotational ductility factor (μ_θ) as a design parameter. It is noted that use of curvature ductility factor (μ_φ), plastic hinge rotations and/or strain values for materials is also feasible, although not done here.

To meet the aforementioned goal, element forces and rotations are first obtained from the results of a standard response spectrum (elastic) analysis. Pier stiffness in this case should be estimated on the basis of yield condition in the pier, preferably by taking into account the effects of axial load ratio; the diagrams proposed in (Priestley et al. 1996) and adopted by Caltrans (Bardakis and Fardis 2011) can be used, considering axial load from service loading, and assuming either minimum reinforcement (1 %) or that resulting from design for non-seismic loading (if higher than 1 %); the diagrams of Fig. 7.8.

Design for flexure is carried out in terms of design values of material strength (in R/C piers f_{cd} and f_{yd} for concrete and steel, respectively) using commonly available design aids. On the other hand, operationality checks (Step 4) are based on the results of inelastic analysis, for which mean values are commonly adopted (f_{cm} and f_{ym}); furthermore, some members are expected to posses overstrength with respect to the design moments used in their dimensioning, due to detailing requirements, i.e. rounding (upwards) of required reinforcement areas and use of minimum reinforcement specified by codes. For these two reasons, the initial elastic analysis should be carried out for an appropriate fraction ν_o of the earthquake level associated with the operationality performance level (e.g. 50 %/50 years). Due to the expected overstrength, the recommended ν_o factor is lower than the ratio of f_{yd}/f_{ym} (equal to 0.79 if the mean yield strength of steel f_{ym} is taken as 10 % higher than the characteristic strength f_{yk}). Furthermore, the ν_o factor should also account for the

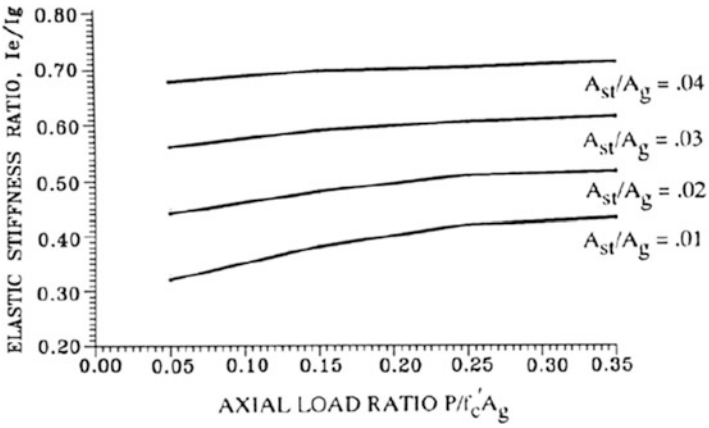

Fig. 7.8 Effective stiffness of cracked reinforced concrete circular sections (Bardakis and Fardis 2011; Priestley et al. 1996)

differences in the moments derived from a response spectrum analysis and those from a series of response history analysis for selected accelerograms (see steps 2 and 4). As an alternative, one could select to use design values of yield moments in the inelastic analysis (a practice not adopted by current codes), in which case a different ν_o factor should be used (note that if $\nu_o = 1$ is selected piers will not yield for the operationality earthquake, which is deemed as a very high performance level, typically not justified in economic terms). It is perhaps worth noting that the problem of mixing design and mean values of material strength is by no means specific to the PBD method presented here; modern codes like Eurocode 8 adopt both elastic and inelastic analysis methods and recommend use of design values for strength verifications and of mean values for displacement or deformation verifications.

Subsequently, elastic rotations (θ_{el}) are related to the corresponding inelastic ones (θ_{inel}), using an empirical procedure (like (Kappos et al. 2012a)); use of empirical factors to estimate θ_{inel} is an inherent limitation of the proposed procedure, since otherwise ductility factors cannot be estimated at this stage. Referring to Fig. 7.9, having defined the target rotational ductility factor (μ_θ) and the maximum inelastic rotation, θ_{inel} (this is the *total* chord rotation, not the plastic one), from the θ_{el} found in the elastic analysis, the yield rotation ($\theta_y = \theta_{inel}/\mu_\theta$) is calculated for every pier. For simplicity of the procedure one could assume first that M-θ response is elastic-perfectly plastic (as in Fig. 7.9) and second that the slopes of the elastic and the elastoplastic M-θ diagrams are the same. Then the corresponding yield moment (M_y) can be easily computed, as the intersection of the elastic part of the diagram and the vertical line drawn at θ_y, as shown in Fig. 7.9; this is the moment to be used for the (flexural) design of the pier. A more accurate, and somewhat more involved, procedure is described in the following.

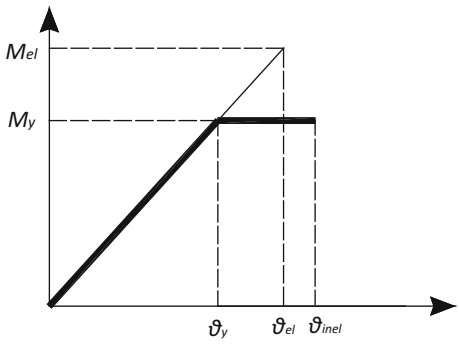

Fig. 7.9 Elastic and elastoplastic M-θ diagram for piers

Attention should be paid to the fact that an increase in deformation does not come with a proportional decrease in design force, i.e. the slope of the first branch in the elastic and the elastoplastic diagram is generally different (Fig. 7.10). The latter derives from the relation of element moments to rotations (M-θ) that is dependent on the loading history (which is non-proportional). Moments and rotations due to permanent loading (gravity and reduced live loads) are first applied and held constant, and any decrease of the elastic forces (M_{el}) should refer to the seismic loading that is applied after the permanent one. Hence, the yield moment should be

$$M_y = M_g + aM_E \tag{7.25}$$

and since the M-θ relationship for seismic loading is linear for elastic behaviour, the reduction factor a is the same for moments and rotations. Knowing the moments developing due to permanent loads (M_g), the values of reduced pier forces for design aM_E can then be determined. As the value of the yield rotation θ_y is already known, as well as the elastic rotations due to seismic loading (θ_E), the value of the reduction factor can be estimated from the following relationship (based on the geometry of Fig. 7.10):

$$\alpha = \frac{\theta_y - \theta_g}{\theta_E} \tag{7.26}$$

The differences in the yield moments resulting from the accurate procedure from those from the simplified one are not large (less than 10 % on the average, but in some instances they are higher, especially for the positive M_y).

According to the aforementioned procedure, the reduced design moments are computed for every pier, and they are directly related to the target rotational ductility selected for the operationality performance level. The longitudinal reinforcement demand for the piers is calculated using standard flexural design procedures and compared to the minimum requirements according to code provisions. In case the longitudinal reinforcement demands are found to be less than the minimum requirements, reduction of cross sections is in order (reduction of stiffness), otherwise deformations for the considered performance level will be less than

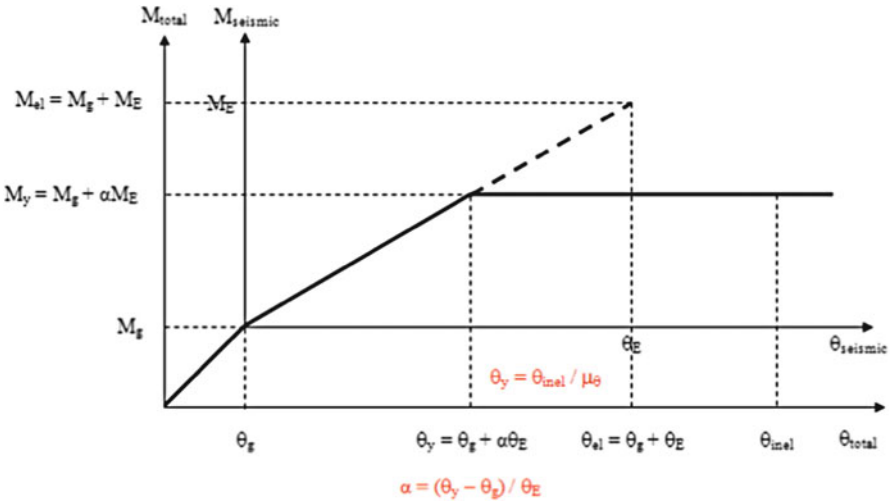

Fig. 7.10 Definition of the correct slope of M- θ_{inel} diagram and of $a\theta_E$

the allowable ones; clearly, this stage involves striking a balance between economy and performance.

Step 2 – Selection of seismic actions. The response-history analysis necessary for seismic design according to the proposed method requires the definition of appropriately selected input seismic motions (see also Sect. 7.2.2). The accelerogram set used for a 3D analysis should include a pair of components for every seismic motion, provided the vertical component is not important for the design of the bridge (which is not always the case). It is recommended that it be selected based on the results of a seismic hazard analysis ('deaggregation' phase, wherein M and R for the site in consideration are determined). Hence the selected input seismic motions should conform to certain criteria concerning magnitude (e.g. $M_s = 6.0–6.5$), and epicentral distance (e.g. $R = 10–25\ km$), and also peak ground acceleration (e.g. $PGA > \sim 0.1\ g$). An additional criterion, not specifically required by Eurocode 8, but important all the same, is the similarity of spectra (those of the selected motions to the target spectrum); software for such multi-criteria selection of the design accelerograms is currently available, e.g. (Katsanos and Sextos 2013).

The earthquake motions used for design, should be properly scaled in order to correspond to the level associated with the limit state examined ('operationality' limit state for the design of energy dissipation zones, and 'life safety' for the other members). Several scaling procedures have been explored (Kappos et al. 2007) and the one adopted by EC8-Part 2 (Kappos et al. 2013) is suggested, modified with regard to the amount the ordinates of the elastic spectrum are exceeded within the critical range of periods, i.e. 10 % instead of 30 % (which is deemed incompatible with the adopted safety format).

Step 3– Set-up of the partially inelastic model. During this step a partially inelastic model (PIM) of the structure is set up, wherein the columns of the piers (top and bottom if they are monolithically connected to the deck) are modelled as yielding elements, with their strength based on the reinforcement calculated for reduced element moments according to the inelastic deformations allowed for the operationality limit state (step 1). In the same model, the remaining parts of the bridge are modelled as elastic members. Since the dissipating zones have been designed for flexure at step 1, the stiffness of the piers can now be estimated from Eqs. (7.1) and (7.2) using the actual yield curvature and yield moment of the pier ends (mean values, since deformations will be checked at this stage).

Step 4 – Serviceability/operationality verifications. The use of inelastic dynamic response-history analysis in the PIM, involves a set of recorded motions scaled to the intensity corresponding to the operationality level. The verifications include specific limits for maximum drifts and plastic deformations of critical members (i.e. the piers). The limits can be derived on the basis of accepted damage, especially in the context of allowing the bridge to remain operational under this level of seismic action. Several criteria are discussed in (fib 2007) and it is clear that the proposals available in the literature vary substantially, from conservative ones (e.g. (Choi et al. 2004) addressing non-seismically designed columns) to very daring ones (Priestley et al. 1996) intended for modern ductile bridge piers. An appropriate way to define acceptable damage for R/C piers is in terms of strains; for instance, it is clear that the functionality of the bridge will not be impaired if cover concrete does not spall, which typically occurs at strains between 3.5 and 4‰. Such strain values can then be used to derive either displacement limits based on simplifying assumptions for the bending moment in the pier (e.g. (Kowalsky 2002)) or moment – rotation diagrams that are more appropriate for the type of analysis used herein. In the case of bridges (and in contrast to normal buildings) deformation control in the piers does not fully guarantee that the bridge will remain functional (operational); it is equally important to check that bearings (which will be present at least in seat-type abutments) also remain functional. For the usual type of elastomeric bearings this limit could be set to between 50 and 100 mm (Choi et al. 2004), or better, in terms of bearing strain, between 0.5 and 1.0. Moreover, the width of joints (in modern bridges normally located at the abutments, except for very long decks) should be selected such that they remain open under this level of seismic action, to avoid damage at the backwalls.

The purpose of this step, apart from checking the inelastic performance of the structural system, is the verification that the required rotational ductility factor (μ_θ) in the piers is consistent with the values considered during the design. Hence, this step is basically an *assessment* (or verification) of the seismic response of the bridge for the 'operationality' level. Since inelastic dynamic analysis is used in order to check the seismic response of the structure for the aforementioned performance level, *mean* values of material strength are considered (f_{cm} and f_{ym} for concrete and steel respectively).

Step 5 – Verifications for the 'life safety' or 'damage limitation' limit state. The design of members (such as the deck or the abutments) considered elastic in setting up the PIM, is verified on the basis of results of inelastic response-history analyses of the aforementioned model for each of the selected sets of input motions properly scaled to the intensity of the earthquake associated with the 'life safety' requirement (probability of exceedance 10 %/50 years, or lower, depending on the importance of the bridge). Equivalently, one can select this as the 'damage limitation' limit state discussed in Sect. 7.3.1, i.e. the extent of damage is such that first it can be repaired after the earthquake (closure of the bridge will be required for a certain period) and second there is no noticeable risk to life due to this damage.

This is an important step for buildings (Kappos and Stefanidou 2010) since several critical elements, in particular the columns (except at the base of the ground storey), are designed at this stage. In the case of bridges, it is very likely that the deck and the abutments will have (from non-seismic load combinations) a higher strength than that required on the basis of this analysis. A notable exception is continuity slabs in decks consisting of precast-prestressed beams with cast in situ top slab (a structure quite different from the box girder bridges that are the focus of this chapter). Such slabs will certainly yield under this level of seismic action, but this is perfectly within the design philosophy of such bridges and is also allowed by the codes (Kappos et al. 2013); there is no need for verification of the plastic rotation either, since the shallow sections of R/C slabs can develop very high rotations without rupture. On the contrary, it is essential that bearing deformations be checked at this stage; allowable values are the same as those discussed in the DDBD procedure described in Sect. 7.3.1 (around 2.0, i.e. strains of 200 % in the elastomer).

Step 6– Design for shear. To account for the less ductile nature of this mode of failure, shear forces should be calculated for seismic actions corresponding to the 2 %/50 years earthquake (associated with the 'collapse prevention' performance level). However, to simplify the design procedure, design and detailing for shear can be carried out using shear forces calculated from inelastic response-history analysis for the seismic action associated with the 'life safety' performance level, and implicitly relate them to those corresponding to the 2 %/50 years earthquake through appropriately selected magnification factors (γ_v). Recommended γ_v factors, accounting mainly for the strain-hardening effect corresponding to higher plastic rotations at this earthquake level, are between 1.15 and 1.20.

Step 7 – Detailing of critical members. Detailing of R/C piers for confinement, anchorages and lap splices, is carried out with due consideration of the expected level of inelasticity. Detailing of piers can be carried out according to the provisions of Chapter 6 of EC8 (Kappos et al. 2013) for ductile members. However, instead of basing the detailing on the default curvature ductilities specified in the Code ($\mu_\varphi = 13$ for bridges of ductile behaviour), the actual μ_φ estimated for the earthquake associated with the collapse prevention requirement are used in this PBD method. This results in both more rational and, as a rule, more economic, detailing

of the piers. Moreover, it should be verified that bearings do not exceed their ultimate deformability, i.e. a strain in the elastomer of around 5.0.

7.5 Seismic Assessment of Bridges

7.5.1 Brief Overview of Available Assessment Procedures

A variety of analytical procedures are currently available for the seismic assessment of structures; the state-of-the-art is quite advanced in the case of buildings for which assessment codes have been developed some time ago, such as Eurocode 8–3 (CEN Techn. Comm. 250/SC8 2005), which however does not cover bridges (this is one of the goals of the evolution of Eurocode 8, that has just started and is expected to last for some years). It has long been recognised that a proper assessment can be carried out only if the post-elastic response of the structure is captured in the analysis, hence revealing the actual plastic mechanism that will develop under a given level of earthquake action. In older and/or poorly designed structures this mechanism can be an unfavourable one, involving concentration of ductility demands in one (or a few) regions; a known example is the case of bridges with significantly unequal heights, wherein a shorter pier is close to the middle of the bridge (such piers yield early on and inelastic deformation tends to concentrate therein).

In the light of the above, leading code-type documents for seismic assessment (of buildings), such as Eurocode 8 – Part 3 (CEN Techn. Comm. 250/SC8 2005) and ASCE 41-06 (ASCE/SEI 2007) recommend and, under specific conditions (such as the presence of irregularities), impose the use of inelastic analysis methods. Both types of inelastic analysis are allowed, but the static (pushover) method is presented in more detail in documents related to seismic assessment, particularly the American ones, such as (ASCE/SEI 2007). Regarding bridges, the most comprehensive document covering assessment is the FHWA Seismic Retrofitting Manual (FHWA 2006). This document includes a number of options for carrying out the analysis of an existing bridge; a total of 4 methods are prescribed, ranging from elastic (static or dynamic) to nonlinear response-history analysis, the applicability of each method depending primarily on the degree of irregularity in the bridge configuration. Interestingly, from a practice perspective, is that there are also options for carrying out a limited assessment of the bridge without any analysis at all, simply by checking the capacity of some critical regions (connections, seat widths) against minimum requirements specified in the Manual. Two options are given for the nonlinear static (pushover) method. The first one (‘D1’) applies to bridge behaving essentially as SDOF systems (this is the case of straight bridges in their longitudinal directions, when piers are monolithically connected to the deck). All other bridges should be analysed using the second method (‘D2’), which combines a response spectrum analysis to assess the displacement demands on

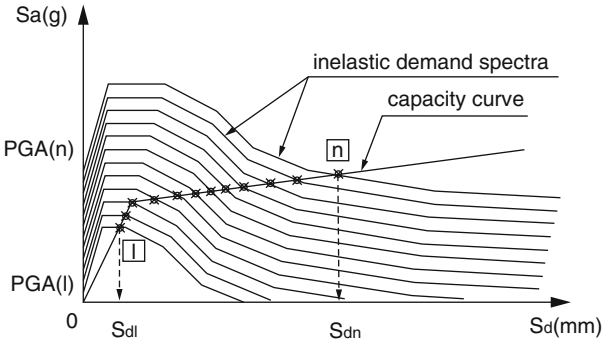

Fig. 7.11 Capacity and demand spectra

the bridge with estimation of capacity through pushover analysis. In both cases the correlation of capacity and demand is made using the capacity spectrum technique (capacity and demand plotted on the same diagram depicting spectral acceleration vs. spectral displacement of an equivalent SDOF system), which has been used for quite some time for buildings following the publication of the ATC-40 Manual (Council 1996). Figure 7.11 shows an example application of this procedure; the demand spectra can be either overdamped elastic spectra as suggested in ATC-40, or proper inelastic spectra as in the figure (Moschonas et al. 2009). It is clear from the figure that the bridge capacity is represented by a single curve, while assessment can be carried out for multiple levels of seismic demand, which is an essential feature of PBD procedures.

The preference of existing codes and guidelines (for both bridges and buildings) for the nonlinear static, as opposed to the nonlinear dynamic, approach should be attributed to the presumption that inelastic static analysis is simpler to apply in practice, which may or may not be true if the limitations of the static method are dully accounted for. More specifically, irregular structural configurations are quite common in both 'old' and new bridges, and irregular structures are typically affected by higher modes and/or by changes in their dynamic characteristics in the post-elastic range of their response to seismic actions. Typical examples are long bridges, and also any size bridges with no transverse restraint of the deck over the abutments, wherein consideration of at least the second mode (in the transverse direction of a bridge) is mandatory. Consideration of multiple loading pattern in pushover analysis (as prescribed in CEN Techn. Comm. 250/SC8 2005; ASCE/SEI 2007 and several other codes) is a mixed blessing, in the sense that higher mode effects can still be missed (especially toward the ends of the bridge), whereas basing the final assessment on an 'envelope' of the action effects derived from each pattern is very often over-conservative. Therefore, use of inelastic dynamic (response-history) analysis is in many respects an appropriate choice and, with the currently available tools (like those in Carr 2006; CSI [Computers and Structures Inc.] 2007) it is also a feasible one. As an alternative, nonlinear static procedures that properly (albeit approximately) account for higher modes effects can be used. A very

promising procedure is the modal pushover method, originally proposed by Chopra and Goel (2002) for buildings and later extended to bridges by Paraskeva and Kappos (Paraskeva and Kappos 2010; Paraskeva et al. 2006); in this method separate pushover analyses are carried out for various modal force patterns and the results are combined statistically, except for forces in the piers that are derived from the pertinent $M - \theta$ (moment vs. rotation) diagrams.

A broader discussion of the 'pros' and 'cons' of the aforementioned procedures and the analytical tools for their implementation can be found in a recent book on inelastic methods for the analysis of bridges (Kappos et al. 2012b). By applying the available methods to a number of case studies it was possible to confirm the range of applicability and the feasibility of each method. Table 7.1 presents in matrix form the recommended type of analysis for the assessment of each type of bridge.

A case study of seismic performance assessment is given in the next section; it concerns the bridge designed in Sect. 7.3, which is assessed using inelastic dynamic (response-history) analysis for a set of ground motions; hence, the case-study also serve for furnishing a good idea of the possibilities of current assessment procedures and the parameters that can (and should) be checked in each case. It is noted that rather than using code-prescribed values, assessment is based herein on state-of-the-art methods for estimating the local (plastic rotation) and global (drift) capacity of R/C bridges.

7.5.2 Assessment of the Bridge Designed to the Displacement-Based Procedure

The standard DDBD and the extended MDDBD procedure (Sect. 7.3.2) were assessed using nonlinear response-history analysis (NLRHA) for artificial records closely matching the design spectrum. Two different evaluation approaches were explored as described in the following.

NLRHA was first applied adopting the same assumptions as in the MDDBD. Therefore, yield curvatures and yield moments equal to the design requirements from Step 8 (i.e. SRSS combination of structural analysis results), were used in conjunction with a zero post-elastic slope of the moment-curvature response of the piers. This approach, hereafter referred to as the NLRHA(EI_{des}) case, was deemed necessary for evaluating the efficiency of the proposed MDDBD disengaged from parameters such as material strengths and final detailing of reinforcement. On the other hand, the second evaluation approach, referred to as the NLRHA(EI_{ass}) case, was meant to assess the (M)DDBD design in terms of the expected actual performance of the bridge under the design seismic actions. In particular, the design was deemed as safe if the displacement ductility demand obtained from NLRHA did not exceed the pier displacement ductility assumed in the design. This deterministic assessment requires an accurate and realistic modelling of the inelastic response to obtain the most probable response quantities. To this purpose, moment-curvature

Table 7.1 Recommended types of inelastic analysis (Kappos et al. 2012b)

Type of bridge	Single-mode methods	Multi-mode methods		Nonlinear response history analysis
		Non-adaptive	Adaptive	
Response is governed predominantly by one mode, which does not considerably change:	X			
Short bridges on moderate to stiff soil, pinned at the abutments, and not supported by very short columns				
The influence of higher modes is limited and their shape does not considerably change when the seismic intensity is increased:	X	X		
Short bridges pinned at the abutments, supported by short side and long central columns				
Considerable influence of higher modes, that do not significantly changed their shape:		X	X	
Long bridges (or curved) without very short central columns				
Considerable influence of one or a few number of modes, which significantly change the shape:			X	
Short bridges with roller supports at the abutments				
Considerable influence of higher modes, which significantly change their shape when the seismic intensity is changed:				X
Short or long bridges supported by very short central and higher side columns				

analyses based on mean values for material properties and the final detailing of reinforcement, were performed for each pier section utilizing the in-house developed computer program RCCOLA.NET. The assessment in both cases focussed mainly on the target-displacement profiles and on design quantities such as yield displacements, displacement ductilities, stiffnesses, and magnitude of forces developed in critical members of the bridge.

Nonlinear analyses were carried out using Ruaumoko3D (Carr 2006); appropriate nonlinear beam members that in general follow the concept of the one-component model, were introduced in the finite element model (Fig. 7.3) to model the inelastic response of the piers (instead of beam-column members, since there are no changes in axial force that affect the yield moments related to the transverse response of this straight bridge). Herein, the modified Takeda degrading-

stiffness hysteresis rules (Carr 2006), (with parameters $\alpha = 0.5$ and $\beta = 0$ as assumed for design (Dwairi and Kowalsky 2006) to estimate ξ_i), were adopted.

Since the primary objective of the assessment was the study of the transverse response of the bridge under a seismic excitation which matches as closely as feasible the 'design excitation' (i.e. the design spectrum), two sets of NLRHA (EI_{des}, EI_{ass}) were performed for each design case (Zone II, III), using five artificial records, generated using the computer program ASING (Sextos et al. 2003) to fit the elastic design S_a spectra. Response history analyses were performed using the unconditionally stable implicit Newmark constant average acceleration method (Carr 2006), while (after some pilot analyses) Rayleigh damping based on tangent stiffness was selected. The integration time step was set equal to 0.01 s, after trial analyses.

In Fig. 7.12 the target-displacement profiles and the displacement profiles obtained from structural analyses within the DDBD and MDDBD procedures are compared with the displacement envelopes from the NLRHA(EI_{des}) and (EI_{ass}) cases; the deck displacements shown in the figures as the NLRHA case are the average of the maximum displacements recorded in the structure during the five RHAs of each set. It is observed that agreement of the DDBD design profiles with the corresponding response-history results is not satisfactory, since the NLRHA profile is closer to the target-displacement profile Δ_i (derived from EMS and accounting for higher mode effects) instead of the displacement profile obtained from structural analysis, on the basis of which design is carried out. On the other hand, the MDDBD target-displacement profiles are closer to that obtained from NLRHA(EI_{des}), more so in the case of Zone II. The main difference between MDDBD and NLRHA(EI_{des}) is noted towards the abutments of the bridge (critical members in design), with differences diminishing in the area of the piers. These differences should be attributed to the inherent inability of elastic design methodologies that are based on modal analysis (e.g. response spectrum analysis) to capture the modification of the dynamic characteristics of the structure during the successive formation of plastic hinges. The MDDBD procedure attempts to capture the maximum probable response at a given performance level (after the formation of plastic hinges) based on a statistical combination (e.g. SRSS) of the peak 'modal' responses.

Additional sets of linear response history analyses (LRHA) for the case '(EI_{des})' were performed to support the above statement. In particular, column stiffnesses were set equal to secant stiffnesses corresponding to maximum displacements obtained from previously run nonlinear analysis (i.e. NLRHA(EI_{des})). The displacement envelopes resulting from these analyses indicate the contribution of the first two modes with similar participation factors as those obtained from the EMS method (Fig. 7.12). The NLRHA(EI_{ass}) case is also given in Fig. 7.12 to underline the divergence (in terms of displacement profiles) arising when pier overstrength, due to the use of mean values for material properties and consideration of strain-hardening of steel reinforcement, is considered.

Similar conclusions are drawn with respect to the other design quantities; yield displacements, displacement ductilities, stiffnesses, ultimate member shears,

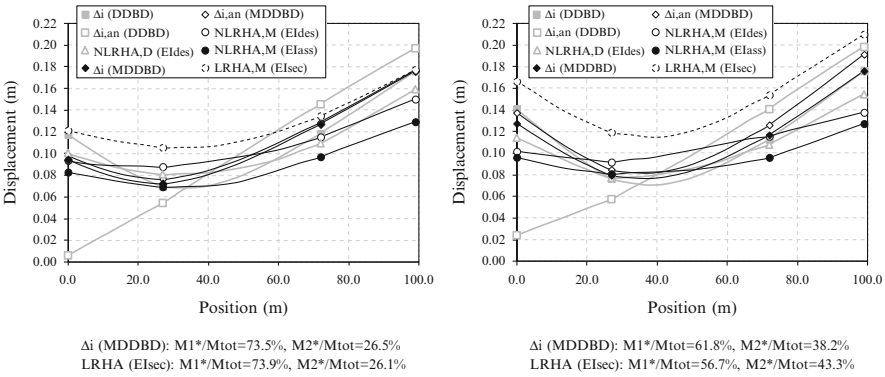

Fig. 7.12 Nonlinear response history maximum displacements for evaluation cases NLRHA (EIdes), (EIass) and linear response history maximum displacements for evaluation case NLRHA(EIdes). *Left*: Zone II; *Right*: Zone III, compared with target-displacements profiles (Δi) and displacement profiles obtained from structural analyses (Δi,an) according to DDBD (D) and Modal DDBD (M)

bearing shear strain and column drift ratios obtained from NLRHA were compared with those estimated at the design stage. Figure 7.13 (supplemented by Table 7.2, as far as the results related to the MDDBD are concerned) illustrates the correlation in the above quantities, for Zone II design. Again, curves shown in the figures as the NLRHA case are the average of the quantities recorded in the structure during the five RHAs, either at the time step each member enters the inelastic range (displacement and shear values at the instant wherein the bending moment at the critical section first reaches the yield bending moment of EI_{des}/EI_{ass} case) or at the time step of maximum response. V-Δ curves shown as MDDBD were drawn based on the assumptions of the method (i.e. assuming zero post-elastic slope of the shear force vs. displacement response and yield displacement according to Eq. (7.14b)) and the results of structural analyses (SRSS combination). It is clear that, contrary to the DDBD, MDDBD predicts very well (i.e. matches closely the values from the NLRHA(EI_{des}) case) the quantities related to member ultimate response (shear forces, displacements and secant stiffnesses at maximum response), which implies the effectiveness of the equivalent cantilever approach in capturing the degree of fixity at the top of the piers, and the base shear distribution approach according to the results of structural analysis. Differences in the quantities related to pier yield are mainly attributed to the estimation of the yield curvature according to the semi-empirical Eq. (7.14b) and the computation of the equivalent cantilever height according to moment diagrams at maximum response instead of the response at the time of yielding. The resulting underestimation of the equivalent cantilever height contributes to underestimation of yield displacements and overestimation of stiffnesses and shears related to pier yield. It is worth mentioning that DDBD yields similar results with MDDBD as far as Column 2 is concerned (whose design is governed by the first mode), whereas it overestimates the 'second mode-based' response of Column 1.

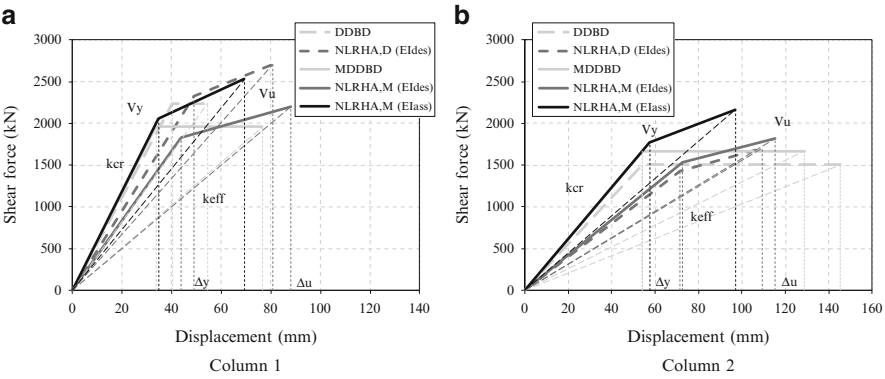

Fig. 7.13 Member shear force vs. displacement curves derived from direct displacement-based design (DDBD), modal direct displacement-based design (MDDBD), and nonlinear response history analyses (NLRHA) for Zone II (PGA = 0.24 *g*) design

As previously mentioned, the results of the NLRHA(EI_{ass}) case were used to verify the reliability of the proposed design method in terms of ductility demand. Both designs were found to be safe, since required ductilities values for Zones II and III are always lower than the design ductilities (see Table 7.2 for case of Zone II). Figure 7.13 also illustrates the effects of overstrength on the V-Δ pier response.

A case study presenting the assessment of the same bridge (T7 overpass) designed according to the deformation-based procedure described in Sect. 7.4.1 can be found in (Gkatzogias and Kappos 2014).

7.6 Closing Remarks

It was attempted to provide here an overview and discussion of the various seismic design procedures available for bridges, with emphasis on new proposals for improved design methods (such as the direct displacement-based and deformation-based design procedures presented herein) and whether they could be useful within the frame of a 'new generation' of codes. As far as the performance of structures designed to current codes is concerned, the answer is straightforward: Far from being perfect (whatever this might mean in the context of practical design), current codes like Eurocode 8 lead to designing robust bridges with ample margins of safety against collapse, and in this respect they are, indeed, adequate. One can argue that sometimes current codes tend to be over-conservative and/or to result in bridge piers that are difficult to detail on-site, but others could argue that earthquakes keep surprising us, in the sense that ground motions stronger than those recorded in the past keep being recorded, hence the extra safety margins apparently provided by current codes should not be reduced.

Table 7.2 Design quantities for the case depicted in Fig. 7.13

Member case	Abutment 1				Abutment 2			Column 1			Column 2	
	MDDBD	NLRHA (EI_{des})	NLRHA (EI_{ass})	MDDBD	NLRHA (EI_{des})	NLRHA (EI_{ass})	MDDBD	NLRHA (EI_{des})	NLRHA (EI_{ass})	MDDBD	NLRHA (EI_{des})	NLRHA (EI_{ass})
Δ_y (mm)							34	44	35	54	73	58
V_y (kN)							1,958.6	1,828.8	2,060.0	1,668.5	1,529.2	1,769.4
Δ_u (mm)	98	94	83	177	141	129	77	88	69	129	115	97
V_u (kN)	491.3	469.0	415.2	885.4	707.7	647.6	1,958.6	2,196.2	2,529.2	1,668.5	1,817.8	2,166.4
K_h (kN/m)	5,011.4	5,011.4	5,011.4	5,011.4	5,011.4	5,011.4						
K_{cr} (kN/m)							58,072.9	41,559.9	59,195.4	30,860.9	21,025.1	30,736.9
K_{eff} (kN/m)							25,576.3	24,984.6	36,493.2	12,952.7	15,774.0	22,342.8
μ_Δ							2.27	2.00	1.99	2.38	1.58	1.68
$\gamma\%$ ($\gamma_u = 2.0$)	1.11	1.06	0.94	2.01	1.60	1.47						
Col drift (%)							1.05	1.21	0.95	1.39	1.24	1.05
h_{eq} (m)							3.43	3.79	4.43	4.39	5.02	5.61

The second question, i.e. whether new performance-based design proposals could or should be incorporated in future seismic codes, is more difficult to answer in a definitive way. Based on the (undoubtedly limited) available evidence, it appears that there are two main issues wherein new proposals can 'entice' code developers: better damage control for a number of different earthquake intensities (in particular those lower that the commonly used single design earthquake with 10 %/50 years probability of exceedance), and, of course, economy. As far as damage control is concerned, the writer's opinion is that the direct deformation-control method (Sect. 7.4) is better suited for inclusion in future codes, not only for 'format' reasons (i.e. that it can be incorporated in existing codes by revising them, rather than by, essentially, completely replacing them), but also because, as already pointed out herein, displacement-based methods, even when applied to structural systems for which they were properly calibrated, do not always guarantee that local inelastic deformations will be within the acceptable limits, since checking of these deformations is not part of the procedure. It is clear, nevertheless, that explicitly checking these local deformations requires more refined and costly types of analysis than the simple equivalent static approach put forward by the DDBD developers. In principle, only inelastic analysis can offer a viable alternative here, and for several types of bridges this analysis should be dynamic (response history) rather than static. Moreover, in many cases, analysis should account not only for inelastic member response but also for (nonlinear) soil-structure interaction effects, a crucial issue that has not been addressed here due to space limitations, but very important in the case of bridges. Of course, as one keeps refining the analysis, the latter is made more complex and difficult to apply in a design office context. Seen from a slightly different perspective, the key difference in the interesting new proposals reviewed here is in the level of approximation, since the goal is common in both of them, i.e. control of damage. The direct DBD procedure assumes that the actual bridge can be properly reduced to an SDOF system (or more systems in the MDDBD method described here) based on a reasonable (inelastic) displacement pattern, whereas the direct deformation-based procedure arrives at the inelastic displacement pattern and the associated local deformations through inelastic analysis, albeit of a reduced inelastic model.

Last and not least, the issue of economy has to be addressed, which is arguably the one most difficult to tackle in a comprehensive way. The available evidence is certainly too limited for drawing conclusions of general validity. Moreover, it should be emphasised that the economy of the final design does not depend solely on the way seismic action is defined and the analysis method used (e.g. code-type or PBD), but on several other issues that have not been studied systematically so far. In view of this paucity of comparative studies, the only definitive conclusion regarding the issue of economy is that additional and, especially, more systematic and comprehensive, studies are required to compare the final products resulting from each procedure, wherein these products should be realistic bridges, representative of the current seismic design practice.

Acknowledgements A number of the author's students have made significant contributions to some of the studies summarised herein. The contribution of K. Gkatzogias, PhD student at City University London, is particularly acknowledged.

References

AASHTO (2011) Guide specifications for LRFD seismic bridge design. AASHTO, Washington, DC

AASHTO [American Association of State Highway and Transportation Officials] (2010) LRFD bridge design specifications, 5th edn. AASHTO, Washington, DC

Adhikari G, Petrini L, Calvi GM (2010) Application of direct displacement based design to long-span bridges. Bull Earthquake Eng 8(4):897–919

Alvarez Botero JC (2004) Displacement-based design of continuous concrete bridges under transverse seismic excitation. M.Sc. dissertation. European school for advanced studies in reduction of seismic risk (Rose School), University of Pavia, Pavia

Applied Technology Council (1996) ATC-40: seismic evaluation and retrofit of concrete buildings. Rep. SSC 96–01, CSSC-ATC, Redwood City

ASCE/SEI (2007) Seismic rehabilitation of existing buildings – ASCE standard 41–06. American Society of Civil Engineers, Reston

Bardakis VG, Fardis MN (2011) A displacement-based seismic design procedure for concrete bridges having deck integral with the piers. Bull Earthquake Eng 9:537–560

Blandon CA, Priestley MJN (2005) Equivalent viscous damping equations for direct displacement-based design. J Earthquake Engineering 9:257–278

Caltrans [California Department of Transportation] (2013) Seismic design criteria ver. 1.7. Caltrans Division of Engineering Services, California, USA

Calvi GM, Kingsley GR (1995) Displacement-based seismic design of multi-degree-of-freedom bridge structures. Earthquake Eng Struct Dyn 24(9):1247–1266

Carr AJ (2006) Ruaumoko 3D: inelastic dynamic analysis program. University of Canterbury, Christchurch

CEN (2004) Eurocode 2: design of concrete structures – part 1: general rules and rules for buildings (EN 1992-1-1). CEN, Brussels

CEN (Comité Europeen de Normalization) (2005) Eurocode 8, design of structures for earthquake resistance – part 2: bridges. CEN, Brussels

CEN Techn. Comm. 250 / SC8 (2005) Eurocode 8: design provisions of structures for earthquake resistance – part 3: assessment and retrofitting of buildings (EN1998-3). CEN, Brussels

Choi E, DesRoches R, Nielson B (2004) Seismic fragility of typical bridges in moderate seismic zones. Eng Struct 26(2):187–199

Chopra AK, Goel RK (2002) A modal pushover analysis procedure for estimating seismic demands for buildings. Earthquake Eng Struct Dyn 31(3):561–582

CSI [Computers and Structures Inc.] (2007) SAP200: three dimensional static and dynamic finite element analysis and design of structures. Computers and Structures Inc., Berkeley

Dwairi H, Kowalsky MJ (2006) Implementation of inelastic displacement patterns in direct displacement-based design of continuous bridge structures. Earthq Spectra 22(3):631–662

Dwairi HM, Kowalsky MJ, Nau JM (2007) Equivalent damping in support of direct displacement-based design. J Earthquake Eng 11:512–530

FHWA [Federal Highway Administration] (2006) Seismic retrofitting manual for highway bridges part 1 – bridges (FHWA- HRT-06-032). Turner-Fairbank Highway Research Center, McLean

fib (2007) Structural solutions for bridge seismic design and retrofit. Fib Bull 39, Lausanne

Fischinger M, Beg D, Isakovic T, Tomazevic M, Zarnic R (2004) Performance based assessment—from general methodologies to specific implementations. International Workshop on PBSD, Bled, Slovenia, pp 293–308 (published in PEER report 2004-05 (UC Berkeley))

Gkatzogias KI, Kappos AJ (2014) Performance-based seismic design of concrete bridges. SECED 2015 conference: earthquake risk and engineering towards a Resilient World, Cambridge UK, 9–10 July 2015

Grant DN, Blandon CA, Priestley MJN (2004) Modeling inelastic response in direct displacement-based design. Report no. ROSE 2004/02, European School of Advanced Studies in Reduction of Seismic Risk, Pavia

Guyader C, Iwan WD (2006) Determining equivalent linear parameters for use in a capacity spectrum method of analysis. J Struct Eng 132(1):59–67

Kappos AJ (2010) Current trends in the seismic design and assessment of buildings: Ch. 11. In: Garevski M, Ansal A (eds) Earthquake engineering in Europe, geotechnical, geological, and earthquake engineering. Springer, Dordrecht

Kappos AJ, Panagopoulos G (2004) Performance-based seismic design of 3D R/C buildings using inelastic static and dynamic analysis procedures. ISET J Earthquake Technol Spec 41 (1):141–158. Issue: Performance-Based Seismic Design (Edited by MJN Priestley)

Kappos AJ, Stefanidou S (2010) A deformation-based seismic design method for 3D R/C irregular buildings using inelastic dynamic analysis. Bull Earthquake Eng 8(4):875–895

Kappos AJ, Goutzika E, Stefanidou S (2007) An improved performance-based design method for 3d R/C buildings using inelastic analysis. ECCOMAS thematic conference on computational methods in structural dynamics and earthquake engineering, paper no. 1375

Kappos AJ, Gidaris I, Gkatzogias KI (2012a) Problems associated with direct displacement-based design of concrete bridges with single-column piers, and some suggested improvements. Bull Earthquake Eng 10(4):1237–1266

Kappos AJ, Saiidi M, Aydinoglu N, Isakovic T (2012b) Seismic design and assessment of bridges: inelastic methods of analysis and case studies. Springer, Dordrecht

Kappos AJ, Gkatzogias KI, Gidaris I (2013) Extension of direct displacement-based design methodology for bridges to account for higher mode effects. Earthquake Eng Struct Dyn 42 (4):581–602

Katsanos EI, Sextos AG (2013) ISSARS: an integrated software environment for structure-specific earthquake ground motion selection. Adv Eng Softw 58:70–85

Katsaras CP, Panagiotakos TB, Kolias B (2009) Effect of torsional stiffness of prestressed concrete box girders and uplift of abutment bearings on seismic performance of bridges. Bull Earthquake Eng 7(2):363–375

Kowalsky MJ (2000) Deformation limit states for circular reinforced concrete bridge columns. J Struct Eng 126(8):869–878

Kowalsky MJ (2002) A displacement-based approach for the seismic design of continuous concrete bridges. Earthquake Eng Struct Dyn 31(3):719–747

Kowalsky MJ, Priestley MJN, MacRae GA (1995) Displacement-based design of RC bridge columns in seismic regions. Earthquake Eng Struct Dyn 24(12):1623–1643

Ministry of Public Works of Greece (2010) Greek seismic code-EAK 2000, Athens, 2000 (amended June, August 2003, March 2010) (in Greek)

Moschonas IF, Kappos AJ, Panetsos P, Papadopoulos V, Makarios T, Thanopoulos P (2009) Seismic fragility curves for Greek bridges: methodology and case studies. Bull Earthquake Eng 7(2):439–468

Ortiz Restrepo JC (2006) Displacement-based design of continuous concrete bridges under transverse seismic excitation. M.Sc. dissertation. European school for advanced studies in reduction of seismic risk (ROSE School), University of Pavia, Pavia

Paraskeva T, Kappos AJ (2010) Further development of a multimodal pushover analysis procedure for seismic assessment of bridges. Earthquake Eng Struct Dyn 39(2):211–222
Paraskeva TS, Kappos AJ, Sextos AG (2006) Extension of modal pushover analysis to seismic assessment of bridges. Earthquake Eng Struct Dyn 35(11):1269–1293
Priestley MJN, Seible F, Calvi GM (1996) Seismic design and retrofit of bridges. Wiley, New York
Priestley MJN, Calvi GM, Kowalsky MJ (2007) Displacement-based seismic design of structures, 1st edn. IUSS Press, Pavia, 720 pp
SEAOC Ad Hoc Committee (1999) Tentative guidelines for performance-based seismic engineering, App. I of: recommended lateral force requirements and commentary. SEAOC, Sacramento
Sextos AG, Pitilakis KD, Kappos AJ (2003) Inelastic dynamic analysis of RC bridges accounting for spatial variability of ground motion, site effects and soil-structure interaction phenomena. Part 1: methodology and analytical tools. Earthquake Eng Struct Dyn; 32(4):607–627
Suarez V, Kowalsky MJ (2007) Displacement-based seismic design of drilled shaft bents with soil-structure interaction. J Earthquake Eng 11(6):1010–1030
Suarez VA, Kowalsky MJ (2010) Direct displacement-based design as an alternative method for seismic design of bridges. In: SP-271CD: structural concrete in performance-based seismic design of bridges CD-ROM. ACI, Farmington Hills, Michigan, USA
Suarez VA, Kowalsky MJ (2011) A stability-based target displacement for direct-displacement-based design of bridge piers. J Earthquake Eng 15(5):754–774
Takeda T, Sozen M, Nielsen N (1970) Reinforced concrete response to simulated earthquakes. J Struct Div ASCE 96(12):2557–2573